

# Sampling-based Stochastic Data-driven Predictive Control under Data Uncertainty

Johannes Teutsch, Sebastian Kerz, Dirk Wollherr, and Marion Leibold

**Abstract**—We present a stochastic output-feedback data-driven predictive control scheme for linear time-invariant systems subject to bounded additive disturbances and probabilistic chance constraints. The approach uses data-driven predictors based on an extension of Willems’ fundamental lemma from behavioral systems theory and a single persistently exciting input-output data trajectory. Compared to current state-of-the-art approaches that rely on availability of exact disturbance data, we deterministically approximate the chance constraints in a sampling-based fashion by leveraging a novel parameterization of the unknown disturbance data trajectory, considering consistency with the measured data and the system class. A robust constraint on the first predicted step guarantees recursive feasibility of the proposed controller as well as constraint satisfaction in closed-loop. We show robust asymptotic stability in expectation under further standard assumptions. A numerical example demonstrates the efficiency of the proposed control scheme.

**Index Terms**—Chance constraints, Data-driven control, Predictive control, Sampling-based chance constraints approximation, Stochastic systems.

## I. INTRODUCTION

Developing safe controllers for autonomous systems in uncertain environments is a demanding task in general. While traditional control methods rely on accurate system models, data-driven approaches have recently received increased interest [1]. When performance criteria and constraints on system variables need to be taken into account, data-driven predictive control (DPC) is a well-suited control approach [2], [3]. As in model predictive control (MPC), DPC repeatedly solves a finite horizon optimal control problem (OCP), applying only the first input of the optimal input sequence at each time-step. The space of all finite length trajectories of a linear time-invariant (LTI) system is searched using a persistently exciting (PE) past input-output data trajectory based on Willems’ fundamental lemma [4], and thus no explicit model is required.

When data are affected by (bounded) measurement noise or additive disturbances, robustified DPC schemes can be used to still provide closed-loop guarantees [5], [6], although at the cost of conservative constraint handling. In contrast to robust schemes, stochastic DPC leverages distributional information of additive disturbances in order to guarantee the satisfaction of probabilistic chance constraints [7], [8], [9].

All authors are with the Chair of Automatic Control Engineering (LSR), Department of Computer Engineering, Technical University of Munich, Theresienstr. 90, 80333 Munich, Germany {johannes.teutsch, s.kerz, dirk.wollherr, marion.leibold}@tum.de

Similar to stochastic MPC [10], the resulting controller leads to enlarged domains of feasibility and less conservative closed-loop behavior, allowing for effective control in applications where infrequent constraint violations can be tolerated.

In literature, there exist stochastic DPC schemes that come with closed-loop certificates for constraint satisfaction and stability: a tube-based approach for systems with full state availability [9], and an output-feedback DPC scheme based on polynomial chaos expansion [8].

However, both mentioned prior works require data of an input-disturbance-state or input-disturbance-output trajectory to exactly represent the dynamics of the disturbed linear system via extensions of the fundamental lemma. In other words, it is assumed that the disturbance in the dynamics can be measured or retroactively estimated at every time-step. Other stochastic DPC schemes in literature are based on a similar assumption: In [11], a DPC scheme for stochastic systems in innovation form is presented, relying on available innovation data for predictions. Authors in [12] present a stochastic DPC scheme for unbounded noise, and [13] show equivalence of stochastic DPC and MPC when data is exact. Despite relying on exact disturbance data, no closed-loop guarantees are provided. Stochastic DPC with closed-loop guarantees based on input-output data alone and under disturbance data uncertainty remains an open challenge, which we address in this work.

The previously discussed literature only considers noise and disturbances that influence the system dynamics linearly. When the influence is nonlinear (e.g., parametric uncertainty), or when uncertainties follow a non-Gaussian distribution, reformulating the stochastic chance constraints into tractable deterministic expressions is challenging. In such cases, sampling-based methods provide simple approaches for the deterministic approximation of chance constraints. A popular approach is known as scenario MPC [14], where the chance constraints are replaced by hard constraints that must be satisfied for a specified number of predicted sample trajectories, resulting from samples of the uncertainty drawn *online* for every MPC iteration. Although the application is simple, the main disadvantages of scenario MPC are 1) high online computational complexity and 2) lack of closed-loop guarantees. To overcome these issues, *offline*-sampling approaches have been proposed that aim to directly obtain a deterministic approximation of the chance constraints using samples of the uncertainty [15], [16]. This allows for reduction of the online computational complexity of the controller, as well as closed-loop guarantees [15], [17]. First attempts to leverage offline-

sampling approaches in the field of stochastic DPC are presented in our previous work [18]. However, a setting without additive disturbances is considered, full state availability is required, and no stability guarantees are provided.

**Contributions:** In this work, we present a novel model-free strategy for stochastic output-feedback DPC of LTI systems subject to bounded additive disturbances, requiring only a single PE input-output data trajectory while no measurements of the disturbance are required. The proposed strategy efficiently handles both data uncertainty and disturbances during the control phase by employing an offline-sampling-based approach similar to [16] to deterministically approximate the chance constraints. This yields a lightweight predictive control scheme and allows for controller design without the restrictive assumption on availability of exact disturbance data [7], [8], [9], [11] or (possibly conservative) upper bounds on the cumulated disturbance data [6].

The idea of our presented approach is to sample *consistent* disturbance data, for which we present a novel parameterization that naturally allows for incorporation of prior model knowledge (e.g., knowledge on structure and bounds of system parameters) into the controller design, if available. By *consistent*, we mean that the disturbance data may have generated the recorded input-output trajectory in conjunction with an LTI system, considering to the assumed disturbance bounds over the whole trajectory. For each sample, we extend the input-output data by the sampled consistent disturbance data trajectory and construct data-driven multi-step predictors as in subspace predictive control (SPC) [19], [20] for the constraint sampling. An additional constraint on the first predicted step guarantees control-theoretic properties such as recursive feasibility and closed-loop constraint satisfaction [15], [17]. Under standard assumptions on stabilizing ingredients, we show robust asymptotic stability in expectation [21] for the closed-loop system using the proposed controller, depending on the probability of infeasibility of a candidate solution as common in sampling-based stochastic MPC [15], [17].

The main contributions are summarized as follows:

- C1: We present a novel parameterization of the unknown disturbance data considering consistency with the measured input-output data and the underlying system class.
- C2: We propose an output-feedback DPC scheme for LTI systems subject to bounded additive disturbances and chance constraints. The scheme is lightweight and recursively feasible, and does not rely on disturbance measurements.
- C3: We prove robust asymptotic stability in expectation for the closed-loop system under the proposed controller.

**Organization of this paper:** In Section II, we introduce the considered problem setup and provide preliminary results on data-driven system representations and DPC. In Section III, we derive a parameterization of the unknown disturbance data considering consistency with the given input-output data and system class, which allows us to handle the data uncertainty in a sampling-based manner. The design steps for the proposed controller are given in Section IV, while its control-theoretic properties are discussed in Section V. Section VI provides a numerical evaluation of the proposed controller and data-driven predictors, before we conclude the work in Section VII.

**Notation:** We write  $\mathbf{0}$  for any zero matrix or vector and  $\mathbf{I}_n$  for the identity matrix of dimension  $n \times n$ . With  $\mathbf{1}_n \in \mathbb{R}^n$ , we denote a column-vector of all ones. We abbreviate the set of integers  $\{a, \dots, b\}$  by  $\mathbb{N}_a^b$ . The Moore-Penrose pseudo-rightinverse of a matrix  $\mathbf{S}$  is defined as  $\mathbf{S}^\dagger := \mathbf{S}^\top (\mathbf{S}\mathbf{S}^\top)^{-1}$ . The probability measure is defined by  $\Pr[\cdot]$ , whereas the expectation operator is denoted as  $\mathbb{E}[\cdot]$ . The matrix  $[\mathbf{S}]_{[a:b]}$  consists of all rows starting from the  $a$ -th row to the  $b$ -th row of the matrix  $\mathbf{S}$ , whereas  $[\mathbf{S}]_a$  denotes the  $a$ -th row/element of the matrix/vector  $\mathbf{S}$ . With  $\mathbf{S}_1 \otimes \mathbf{S}_2$ , we denote the Kronecker product of the matrices  $\mathbf{S}_1, \mathbf{S}_2$ . For any sequence of vectors  $\mathcal{S}_T = \{\mathbf{s}_i\}_{i=1}^T$ ,  $T \in \mathbb{N}$ , the corresponding Hankel matrix  $\mathbf{H}_L(\mathcal{S}_T)$  of order  $L \leq T$  is defined as

$$\mathbf{H}_L(\mathcal{S}_T) := \begin{bmatrix} \mathbf{s}_1 & \mathbf{s}_2 & \cdots & \mathbf{s}_{T-L+1} \\ \mathbf{s}_2 & \mathbf{s}_3 & \cdots & \mathbf{s}_{T-L+2} \\ \vdots & \vdots & \ddots & \vdots \\ \mathbf{s}_L & \mathbf{s}_{L+1} & \cdots & \mathbf{s}_T \end{bmatrix}. \quad (1)$$

By  $\text{col}(\mathbf{s}_a, \dots, \mathbf{s}_b) := [\mathbf{s}_a^\top, \dots, \mathbf{s}_b^\top]^\top$ , we denote the result from stacking the vectors/matrices  $\mathbf{s}_a, \dots, \mathbf{s}_b$ . For a matrix  $\mathbf{S}$ , we define the weighted 2-norm of the vector  $\mathbf{s}$  as  $\|\mathbf{s}\|_{\mathbf{S}} := \sqrt{\mathbf{s}^\top \mathbf{S} \mathbf{s}}$ . For the Euclidean norm  $\|\mathbf{s}\|$ , we omit the subscript  $\mathbf{S} = \mathbf{I}$ . We write  $\mathbf{y}_{i|k}$  for the predicted output  $i$  steps ahead of time-step  $k$ . For any sets  $\mathbb{S}_1, \mathbb{S}_2$ , we write the Minkowski set addition as  $\mathbb{S}_1 \oplus \mathbb{S}_2 = \{\mathbf{s}_1 + \mathbf{s}_2 \mid \mathbf{s}_1 \in \mathbb{S}_1, \mathbf{s}_2 \in \mathbb{S}_2\}$ , the Pontryagin set difference as  $\mathbb{S}_1 \ominus \mathbb{S}_2 = \{\mathbf{s}_1 \in \mathbb{S}_1 \mid \mathbf{s}_1 + \mathbf{s}_2 \in \mathbb{S}_2 \forall \mathbf{s}_2 \in \mathbb{S}_2\}$ , and set multiplication as  $\mathbf{K}\mathbb{S}_1 = \{\mathbf{K}\mathbf{s} \mid \mathbf{s} \in \mathbb{S}_1\}$ . Positive definiteness of a matrix  $\mathbf{S}$  is denoted by  $\mathbf{S} \succ \mathbf{0}$ , and  $\text{conv}(\cdot)$  denotes the convex hull over a set of vertices. We denote the maximum and minimum eigenvalue of a matrix  $\mathbf{S}$  as  $\lambda_{\max}(\mathbf{S})$  and  $\lambda_{\min}(\mathbf{S})$ , respectively. A function  $\varrho : \mathbb{R}_{\geq 0} \rightarrow \mathbb{R}_{\geq 0}$  is of class  $\mathcal{K}$  if  $\varrho$  is continuous, strictly increasing, and  $\varrho(0) = 0$ . If  $\varrho \in \mathcal{K}$  is unbounded, then  $\varrho$  is of class  $\mathcal{K}_\infty$ . A function  $\beta : \mathbb{R}_{\geq 0} \times \mathbb{R}_{\geq 0} \rightarrow \mathbb{R}_{\geq 0}$  is of class  $\mathcal{KL}$  if  $\beta(\cdot, t) \in \mathcal{K}$  for fixed  $t$  and  $\delta(r, \cdot)$  is continuous, strictly decreasing, and  $\lim_{t \rightarrow \infty} \delta(r, t) = 0$  for fixed  $r$ .

## II. PROBLEM SETUP & PRELIMINARIES

In this section, we first introduce the problem setup consisting of the considered system class and relevant assumptions. Then, we present preliminaries on data-driven system representations based on Willems' fundamental lemma [4] and the DPC framework on which we base our proposed method.

### A. Problem Setup

We consider a discrete-time LTI system  $\Sigma$  of order  $n$  in AutoRegressive with eXtra input (ARX) form with unknown system matrices  $\Phi, \Psi$  and additive disturbance, i.e.,

$$\mathbf{y}_k = \Phi \xi_k + \Psi \mathbf{u}_k + \mathbf{d}_k. \quad (2)$$

System (2) consists of the output  $\mathbf{y}_k \in \mathbb{R}^p$ , input  $\mathbf{u}_k \in \mathbb{R}^m$ , additive disturbance  $\mathbf{d}_k \in \mathbb{R}^p$ , and the vector of past  $T_p \in \mathbb{N}$  inputs and outputs (denoted as the *extended state*)

$$\xi_k := \begin{bmatrix} \text{col}(\mathbf{u}_{k-T_p}, \dots, \mathbf{u}_{k-1}) \\ \text{col}(\mathbf{y}_{k-T_p}, \dots, \mathbf{y}_{k-1}) \end{bmatrix} \in \mathbb{R}^{n_\xi}, \quad n_\xi := (m+p)T_p. \quad (3)$$

We rely on the following assumption on the controllability of an equivalent minimal state-space realization of (2).

**Assumption 1 (Minimal state-space representation)** *There exists a minimal state-space representation of the form*

$$\mathbf{x}_{k+1} = \mathbf{A}\mathbf{x}_k + \mathbf{B}\mathbf{u}_k + \mathbf{E}\mathbf{d}_k, \quad (4a)$$

$$\mathbf{y}_k = \mathbf{C}\mathbf{x}_k + \mathbf{D}\mathbf{u}_k + \mathbf{d}_k, \quad (4b)$$

with controllable  $(\mathbf{A}, \mathbf{B})$  and observable  $(\mathbf{A}, \mathbf{C})$ , such that for some given initial conditions  $\mathbf{x}_0, \boldsymbol{\xi}_0$  and disturbances  $\mathbf{d}_k$ ,  $k \geq 0$ , the input-output trajectories of (2) and (4) coincide.

**Remark 1** *Details on how to construct the system parameters in (4) from  $\Phi$  and  $\Psi$  in (2) are given in [8], [22]. With Assumption 1, a stabilizable and detectable (but not necessarily minimal) state-space representation of (2) is given by [23]*

$$\boldsymbol{\xi}_{k+1} = \tilde{\mathbf{A}}\boldsymbol{\xi}_k + \tilde{\mathbf{B}}\mathbf{u}_k + \tilde{\mathbf{E}}\mathbf{d}_k, \quad (5a)$$

$$\mathbf{y}_k = \Phi\boldsymbol{\xi}_k + \Psi\mathbf{u}_k + \mathbf{d}_k, \quad (5b)$$

with the extended state  $\boldsymbol{\xi}_k$  defined in (3) and the matrices  $\tilde{\mathbf{A}} := \text{col}(\tilde{\mathbf{A}}, \Phi)$ ,  $\tilde{\mathbf{B}} := \text{col}(\tilde{\mathbf{B}}, \Psi)$ ,  $\tilde{\mathbf{E}} := \text{col}(\mathbf{0}, \mathbf{I}_p)$ , where

$$\tilde{\mathbf{A}} := \begin{bmatrix} \mathbf{0} & \mathbf{I}_{(T_p-1)m} & \mathbf{0} & \mathbf{0} \\ \mathbf{0} & \mathbf{0} & \mathbf{0} & \mathbf{0} \\ \mathbf{0} & \mathbf{0} & \mathbf{0} & \mathbf{I}_{(T_p-1)p} \end{bmatrix}, \tilde{\mathbf{B}} := \begin{bmatrix} \mathbf{0} \\ \mathbf{I}_m \\ \mathbf{0} \end{bmatrix}. \quad (6)$$

The equivalent state-space form (5) of (2) allows for simpler analysis of closed-loop properties (see Section V).

The disturbance  $\mathbf{d}_k$  in (2) is subject to the following assumption on its bounds and probability distribution.

**Assumption 2 (Disturbance bounds and distribution)**

*The disturbance  $\mathbf{d}$  is the realization of a zero-mean random variable that is independent and identically distributed (iid) according to a known probability distribution function  $\mathbf{f}_d(\cdot)$  and supported by a known compact polytopic set*

$$\mathbb{D} = \{\mathbf{d} \in \mathbb{R}^p \mid \mathbf{G}_d\mathbf{d} \leq \mathbf{g}_d\} \quad (7)$$

containing the origin.

Furthermore, system (2) is subject to probabilistic output and hard input constraints for all time-steps  $k \geq 0$ , given as

$$\Pr[\mathbf{y}_k \in \mathbb{Y}] \geq 1 - \varepsilon, \quad \mathbb{Y} = \{\mathbf{y} \in \mathbb{R}^p \mid \mathbf{G}_y\mathbf{y} \leq \mathbf{g}_y\}, \quad (8a)$$

$$\mathbf{u}_k \in \mathbb{U}, \quad \mathbb{U} = \{\mathbf{u} \in \mathbb{R}^m \mid \mathbf{G}_u\mathbf{u} \leq \mathbf{g}_u\}, \quad (8b)$$

where  $\mathbb{Y}$  and  $\mathbb{U}$  are compact sets containing the origin.

The objective of the predictive controller is to minimize in a receding horizon fashion the expected finite horizon cost

$$J_{T_f} := \mathbb{E} \left[ \sum_{l=0}^{T_f-1} \left( \|\mathbf{y}_{l|k}\|_Q^2 + \|\mathbf{u}_{l|k}\|_R^2 \right) + \|\boldsymbol{\xi}_{T_f|k}\|_P^2 \right], \quad (9)$$

with weighting matrices  $\mathbf{Q}, \mathbf{R}, \mathbf{P} \succ \mathbf{0}$  and prediction horizon  $T_f \in \mathbb{N}$ .

Since the system matrices  $\Phi$  and  $\Psi$  in (2) are unknown in our problem setting, the model (2) cannot be used for predictions. Instead, we will use data-driven predictions for which we assume to have access to a PE input-output data

trajectory, collected offline before the control phase. Consider the following standard definition of persistency of excitation.

**Definition 1 (Persistency of excitation [4])** *A trajectory  $\mathcal{S}_T = \{\mathbf{s}_i\}_{i=1}^T$  of length  $T \in \mathbb{N}$  with  $\mathbf{s}_i \in \mathbb{R}^{n_s}$  is PE of order  $L \leq T$  if the Hankel matrix  $\mathbf{H}_L(\mathcal{S}_T)$  has full rank  $n_s L$ .*

**Assumption 3 (Persistently exciting data trajectory)** *An input-output trajectory  $\{\mathbf{u}_i^d\}_{i=-T_p+1}^T, \{\mathbf{y}_i^d\}_{i=-T_p+1}^T$  generated by system (2) is available, yielding  $\mathcal{U}_T := \{\mathbf{u}_i^d\}_{i=1}^T, \mathcal{Y}_T := \{\mathbf{y}_i^d\}_{i=1}^T$ , and  $\mathcal{X}_T := \{\boldsymbol{\xi}_i^d\}_{i=1}^T$  via (3). The trajectory of generalized inputs  $\{\text{col}(\mathbf{u}_i^d, \mathbf{d}_i^d)\}_{i=1}^T$  is PE of order  $n + T_f + T_p$ , with system order  $n$  and prediction horizon  $T_f \in \mathbb{N}$ . The corresponding disturbance data trajectory  $\mathcal{D}_T := \{\mathbf{d}_i^d\}_{i=1}^T$  is unknown but satisfies Assumption 2.*

**Remark 2** *Assumption 3 is not restrictive in practice, since appropriate inputs  $\mathbf{u}_i^d$  can be chosen for the offline data collection, and  $\mathbf{d}_i^d$  is the realization of an iid random process (see Assumption 2). Furthermore, we remark that persistency of excitation of order  $n + T_f + T_p$  is sufficient for persistency of excitation of orders smaller than  $n + T_f + T_p$  [4].*

This paper aims to solve the following problem.

**Problem 1** *Given system (2) subject to Assumption 1 with unknown system matrices, and a PE input-output data trajectory as in Assumption 3, design a lightweight output-feedback predictive control scheme that minimizes cost (9) in receding horizon fashion while guaranteeing satisfaction of constraints (8) during closed-loop operation. Constraint satisfaction entails the satisfaction of chance constraints (8a) based on probabilistic knowledge of the disturbance (Assumption 2).*

**Remark 3** *Although we assume that the system matrices in (2) are fully unknown in general, we describe how prior (partial) model knowledge can be incorporated in the controller design in Section III-C.*

In order to address Problem 1, we make use of a data-driven system representation for model-free predictions, as we discuss in the following subsection.

## B. Data-driven System Representations

The following result, known as Willems' *fundamental lemma* [4], stems from behavioral systems theory and allows for a non-parametric representation of (2) directly based on input-output data.

**Lemma 1 (Willems' lemma [4])** *Consider an undisturbed, controllable LTI system  $\Sigma$  of the form (4) with  $\mathbf{d}_k = \mathbf{0}$  and a measured data trajectory  $\mathcal{U}_T, \mathcal{Y}_T$ , and  $\mathcal{X}_T$  ( $\mathcal{D}_T = \{\mathbf{0}, \dots, \mathbf{0}\}$ , cf. Assumption 3) where  $T \geq T_p + T_f$ ,  $T_f \in \mathbb{N}$ , and  $T_p \geq \text{lag}(\Sigma)$  holds<sup>1</sup>. If  $\mathcal{U}_T$  is PE of order  $n + T_p + T_f$ , then any  $(T_p + T_f)$ -length input-output trajectory  $\{\mathbf{u}_i\}_{i=k-T_p}^{k+T_f-1}, \{\mathbf{y}_i\}_{i=k-T_p}^{k+T_f-1}$  is a*

<sup>1</sup> $\text{lag}(\Sigma)$  of an LTI system  $\Sigma$  of order  $n$  is defined as the smallest natural number  $j \leq n$  for which the matrix  $\text{col}(\mathbf{C}, \mathbf{C}\mathbf{A}, \dots, \mathbf{C}\mathbf{A}^{j-1})$  has rank  $n$ .

valid trajectory of  $\Sigma$  for  $k \geq 0$  if and only if there exists  $\alpha \in \mathbb{R}^{T-L+1}$  such that

$$\begin{bmatrix} \xi_k \\ \text{col}(\mathbf{u}_k, \dots, \mathbf{u}_{k+T_f-1}) \\ \text{col}(\mathbf{y}_k, \dots, \mathbf{y}_{k+T_f-1}) \end{bmatrix} = \begin{bmatrix} \mathbf{H}_1(\mathcal{X}_{T-T_f+1}) \\ \mathbf{H}_{T_f}(\mathcal{U}_T) \\ \mathbf{H}_{T_f}(\mathcal{Y}_T) \end{bmatrix} \alpha, \quad (10)$$

with  $\xi_k$  and  $\mathcal{X}_{T-T_f+1} = \{\xi_i^d\}_{i=1}^{T-T_f+1}$  according to (3).

Lemma 1 lays the foundation for describing system behavior without model-knowledge in this work: equation (10) functions as a non-parametric representation of system (4) with  $\mathbf{d}_k = \mathbf{0}$ , e.g., in predictive control schemes [3], [5]. Note that the past input-output trajectory  $\{\mathbf{u}_i\}_{i=k-T_p}^{k-1}$ ,  $\{\mathbf{y}_i\}_{i=k-T_p}^{k-1}$  is used in (10) as the extended state  $\xi_k$  to implicitly fix the initial state of the system in order to retrieve uniquely determined predictions [24]. Lemma 1 only considers deterministic, disturbance-free LTI systems (i.e.,  $\mathbf{d}_k = \mathbf{0}$ ), but by treating the disturbance as an additional input to the system, Lemma 1 extends to systems of the form (4) as follows (cf. [7], [9]).

**Lemma 2 (Extended fundamental lemma)** *Consider a disturbed, controllable LTI system  $\Sigma$  of the form (4) and a measured data trajectory  $\mathcal{U}_T, \mathcal{D}_T, \mathcal{Y}_T$ , and  $\mathcal{X}_T$  ( $\mathcal{D}_T$  is known, cf. Assumption 3) where  $T \geq T_p + T_f$ ,  $T_f \in \mathbb{N}$ , and  $T_p \geq \text{lag}(\Sigma)$  holds. If the trajectory of generalized inputs  $\{\text{col}(\mathbf{u}_i^d, \mathbf{d}_i^d)\}_{i=1}^T$  is PE of order  $n + T_p + T_f$ , then any  $(T_p + T_f)$ -length input-disturbance-output trajectory  $\{\mathbf{u}_i\}_{i=k-T_p}^{k+T_f-1}$ ,  $\{\mathbf{d}_i\}_{i=k}^{k+T_f-1}$ ,  $\{\mathbf{y}_i\}_{i=k-T_p}^{k+T_f-1}$  is a valid trajectory of  $\Sigma$  for  $k \geq 0$  if and only if there exists  $\alpha \in \mathbb{R}^{T-L+1}$  such that*

$$\begin{bmatrix} \xi_k \\ \text{col}(\mathbf{u}_k, \dots, \mathbf{u}_{k+T_f-1}) \\ \text{col}(\mathbf{d}_k, \dots, \mathbf{d}_{k+T_f-1}) \\ \text{col}(\mathbf{y}_k, \dots, \mathbf{y}_{k+T_f-1}) \end{bmatrix} = \begin{bmatrix} \mathbf{H}_1(\mathcal{X}_{T-T_f+1}) \\ \mathbf{H}_{T_f}(\mathcal{U}_T) \\ \mathbf{H}_{T_f}(\mathcal{D}_T) \\ \mathbf{H}_{T_f}(\mathcal{Y}_T) \end{bmatrix} \alpha, \quad (11)$$

with  $\xi_k$  and  $\mathcal{X}_{T-T_f+1} = \{\xi_i^d\}_{i=1}^{T-T_f+1}$  according to (3).

Equivalent versions of Lemma 2 were exploited in recent works for stochastic DPC, such as in [9] for state-feedback tube-based predictive control, and in [8] for output-feedback predictive control based on polynomial chaos expansion. In general, Lemma 2 allows for the formulation of a data-driven OCP where (11) replaces the prediction model and  $\alpha$  acts as a decision variable, implicitly determining input and output trajectories. However, crucially, the system representation (11) relies on the availability of disturbance data  $\mathcal{D}_T$ . If no measurement of the disturbance trajectory is available, e.g., due to lack of appropriate sensors,  $\mathcal{D}_T$  may be estimated from inputs and outputs [7]. However, if the estimates are not exact, the guarantees of Lemma 2 are lost: the right hand side of (11) might produce trajectories that are not realizable by the system.

### C. Data-driven Predictive Control

In order to address Problem 1, we will here formulate the corresponding OCP that acts as the basis of the proposed predictive controller. In order to obtain a tractable OCP that can handle the presence of disturbances, we decompose the

control input into a pre-stabilizing extended state feedback term with gain  $\mathbf{K}$  and a correction term  $\mathbf{v}_k$ , i.e.,

$$\mathbf{u}_k = \mathbf{K}\xi_k + \mathbf{v}_k, \quad (12)$$

where only the latter is determined by the predictive controller. The gain  $\mathbf{K}$  can be determined purely from data, see [5], [25], or Appendix I. In order to reflect this change of inputs, we construct the data  $\mathcal{V}_T := \{\mathbf{v}_i^d\}_{i=1}^T$ ,  $\mathbf{v}_i^d = \mathbf{u}_i^d - \mathbf{K}\xi_i^d$ . Based on the data-driven system representation (11), the OCP associated to the proposed DPC scheme is

$$\underset{\alpha}{\text{minimize}} \quad J_{T_f}(\mathbf{u}_{f,k}, \mathbf{y}_{f,k}) \quad (13a)$$

$$\text{s.t.} \quad \begin{bmatrix} \xi_k \\ \mathbf{v}_{f,k} \\ \mathbf{d}_{f,k} \\ \mathbf{y}_{f,k} \end{bmatrix} = \begin{bmatrix} \mathbf{H}_1(\mathcal{X}_{T-T_f+1}) \\ \mathbf{H}_{T_f}(\mathcal{V}_T) \\ \mathbf{H}_{T_f}(\mathcal{D}_T) \\ \mathbf{H}_{T_f}(\mathcal{Y}_T) \end{bmatrix} \alpha, \quad (13b)$$

$$\Pr[\mathbf{y}_{l|k} \in \mathbb{Y}] \geq 1 - \varepsilon \quad \forall l \in \mathbb{N}_0^{T_f-1}, \quad (13c)$$

$$\mathbf{u}_{l|k} = \mathbf{v}_{l|k} + \mathbf{K}\xi_{l|k} \in \mathbb{U} \quad \forall l \in \mathbb{N}_0^{T_f-1}, \quad (13d)$$

$$\xi_{T_f|k} \in \mathbb{X}_{T_f}, \quad (13e)$$

with the vectors  $\mathbf{v}_{f,k} := \text{col}(\mathbf{v}_{0|k}, \dots, \mathbf{v}_{T_f-1|k})$ ,  $\mathbf{u}_{f,k} := \text{col}(\mathbf{u}_{0|k}, \dots, \mathbf{u}_{T_f-1|k})$ ,  $\mathbf{d}_{f,k} := \text{col}(\mathbf{d}_k, \dots, \mathbf{d}_{k+T_f-1})$ ,  $\mathbf{y}_{f,k} := \text{col}(\mathbf{y}_{0|k}, \dots, \mathbf{y}_{T_f-1|k})$ , the predicted extended state  $\xi_{l|k}$  constructed via (3), and a suitable robust positive invariant (RPI), polytopic terminal constraint set  $\mathbb{X}_{T_f} := \{\xi \in \mathbb{R}^{n\varepsilon} \mid \tilde{\mathbf{G}}\xi \leq \tilde{\mathbf{g}}\}$  designed for stability and constructed from data (see Section V-B and Appendix I).

**Remark 4** *It is implicitly assumed that the data of correction inputs  $\mathcal{V}_T$  satisfies the persistency of excitation condition in Lemma 2, which is almost surely the case for data satisfying Assumption 3. Alternatively, the input decomposition (12) with feedback gain  $\mathbf{K}$  can directly be considered in the data collection to ensure PE data, e.g., as in [6].*

OCP (13) is not solvable in its current form, since the disturbance data  $\mathcal{D}_T$  are unknown and the probabilistic constraint (13c) is intractable due to uncertain  $\mathbf{d}_{f,k}$ . We overcome these issues in three steps: First, we explicitly parameterize the unknown disturbance data  $\mathcal{D}_T$  by considering consistency with the assumed disturbance bounds in Assumption 2 and with the given input-output data in the sense that the resulting input-disturbance-output trajectory could have been generated by an LTI system (2). Second, using the previous parameterization and Assumption 2, we retrieve a set of consistent disturbance data. Finally, using samples of the uncertainties  $\mathcal{D}_T$  (drawn from the set of consistent disturbance data) and  $\mathbf{d}_{f,k}$ , we deterministically approximate the probabilistic constraint (13c). In contrast, existing literature on stochastic DPC applies maximum likelihood estimation or least-squares regression to retrieve *one* (consistent) realization of  $\mathcal{D}_T$  [7], [11] if measurements are not available, and thus loses validity of theoretical guarantees if the estimation is inexact.

Before we present our proposed sampling-based control scheme, in the next section, we discuss how to retrieve a set of consistent disturbance data from the available input-output data in order to render OCP (13) tractable.

### III. CONSISTENCY OF DISTURBANCE DATA

In this section, we will first derive an explicit parameterization of the unknown disturbance data  $\mathcal{D}_T$  considering consistency with the given input-output data  $\mathcal{U}_T, \mathcal{Y}_T$ . Then, we will derive a set of consistent disturbance data that can be further utilized for sampling.

#### A. Consistent Disturbance Data

With data from Assumption 3, let us consider the matrices

$$\begin{aligned} \mathbf{H}_1(\mathcal{X}_T) &= [\boldsymbol{\xi}_1^d \ \cdots \ \boldsymbol{\xi}_T^d], \quad \mathbf{H}_1(\mathcal{Y}_T) = [\mathbf{y}_1^d \ \cdots \ \mathbf{y}_T^d], \\ \mathbf{H}_1(\mathcal{U}_T) &= [\mathbf{u}_1^d \ \cdots \ \mathbf{u}_T^d], \quad \mathbf{H}_1(\mathcal{D}_T) = [\mathbf{d}_1^d \ \cdots \ \mathbf{d}_T^d]. \end{aligned}$$

As the given input-output data  $\mathcal{U}_T, \mathcal{Y}_T$  and unknown disturbance data  $\mathcal{D}_T = \{\mathbf{d}_1^d, \dots, \mathbf{d}_T^d\}$  stem from system (2), the above data matrices must satisfy

$$\mathbf{H}_1(\mathcal{Y}_T) = \Phi \mathbf{H}_1(\mathcal{X}_T) + \Psi \mathbf{H}_1(\mathcal{U}_T) + \mathbf{H}_1(\mathcal{D}_T). \quad (14)$$

Equation (14) allows for the definition of a constraint on the disturbance data  $\mathcal{D}_T$  which guarantees consistency with the given input-output data  $\mathcal{U}_T, \mathcal{Y}_T$  and the underlying system class (2), as presented in [7], [26], [27]. In order to do so, the data must satisfy the following mild assumption [8].

**Assumption 4 (Data requirement)** *The data matrix  $\mathbf{S} := \text{col}(\mathbf{H}_1(\mathcal{X}_T), \mathbf{H}_1(\mathcal{U}_T)) \in \mathbb{R}^{(n_\xi+m) \times T}$  is of full row-rank.*

**Remark 5** *In the present setting, Assumption 4 is mild since the input-output trajectory is randomly perturbed by disturbances at each time-step (see Assumption 3) [8]. In a disturbance-free setting, Assumption 4 is restrictive. A sufficient condition for Assumption 4 in the disturbance-free case is given by  $pT_p = n$  [28, Lemma 13], where  $n$  is the order of the minimal system (4). For small disturbance levels and thus nearly singular  $\mathbf{S}$ , the approach presented in the following will face numerical issues. We remark that in the case of input-state data, this issue vanishes when replacing extended state data with state data: full row-rank of  $\mathbf{S}$  then follows directly from persistency of excitation of the input signal [25] and is independent of the disturbance level.*

**Proposition 1 (Consistency constraint [7])** *Consider data trajectories  $\mathcal{U}_T, \mathcal{D}_T, \mathcal{Y}_T$  of system (2) with unknown  $\mathcal{D}_T$ , satisfying Assumptions 3 and 4. Then,*

$$(\mathbf{H}_1(\mathcal{Y}_T) - \mathbf{H}_1(\mathcal{D}_T)) \Pi_S = \mathbf{0} \quad (15)$$

holds, with  $\Pi_S := \mathbf{I}_T - \mathbf{S}^\dagger \mathbf{S}$ .

Furthermore, any  $\mathcal{D}_T$  satisfying (15) implicitly determines system parameters  $\Phi, \Psi$  of an LTI system (2) such that (14) is satisfied for given  $\mathcal{U}_T, \mathcal{Y}_T$ :

$$[\Phi \ \Psi] = (\mathbf{H}_1(\mathcal{Y}_T) - \mathbf{H}_1(\mathcal{D}_T)) \mathbf{S}^\dagger. \quad (16)$$

**Definition 2 (Consistent disturbance trajectories)** *Given input-output data as in Assumption 3, any disturbance trajectory  $\mathcal{D}_T$  is called consistent if it satisfies (15).*

Under the given assumptions, equation (15) admits infinitely many solutions  $\mathcal{D}_T$ . The following proposition provides an

explicit parameterization of these solutions in terms of  $p(n_\xi + m)$  free parameters, namely the first  $n_\xi + m$  disturbances in the data  $\mathcal{D}_{n_\xi+m} = \{\mathbf{d}_1^d, \dots, \mathbf{d}_{n_\xi+m}^d\}$ .

**Proposition 2 (Consistency parameterization)** *Consider an input-output data trajectory  $\mathcal{U}_T, \mathcal{Y}_T$  of system (2) satisfying Assumptions 3 and 4 with  $\mathcal{D}_T$  unknown. A candidate disturbance trajectory  $\mathcal{D}_T$  is consistent if and only if*

$$\mathbf{H}_1(\mathcal{D}_T) = \Gamma_1 + \mathbf{H}_1(\mathcal{D}_{n_\xi+m}) \Gamma_2, \quad (17)$$

where  $\Gamma_1$  and  $\Gamma_2$  are matrices (defined below) that depend solely on the input-output data  $\mathcal{U}_T, \mathcal{Y}_T$ .

*Proof:* Since  $\mathbf{S} = \text{col}(\mathbf{H}_1(\mathcal{X}_T), \mathbf{H}_1(\mathcal{U}_T))$  has full row-rank  $n_\xi + m$  by Assumption 4, the solutions  $\mathcal{D}_T$  of (15) satisfy

$$\mathbf{H}_1(\mathcal{D}_T) = \mathbf{H}_1(\mathcal{Y}_T) \Pi_S + \Delta \Pi_S^0, \quad (18)$$

where  $\mathbf{H}_1(\mathcal{Y}_T) \Pi_S$  is the least-squares solution of (15), the matrix  $\Delta \in \mathbb{R}^{p \times (n_\xi+m)}$  contains free parameters, and  $\Pi_S^0 \in \mathbb{R}^{(n_\xi+m) \times T}$  is chosen such that  $\text{im}(\Pi_S^{0\top}) = \ker(\Pi_S)$ , e.g.,  $\Pi_S^0 = \mathbf{S}$ . We now want to express  $\Delta$  in terms of  $\mathcal{D}_{n_\xi+m}$ . Consider the first  $n_\xi + m$  columns of (18) and denote the matrices that consist of the first  $n_\xi + m$  columns of  $\mathbf{H}_1(\mathcal{Y}_T) \Pi_S$  and  $\Pi_S^0$  as  $\tilde{\mathbf{H}}^{\text{LS}}$  and  $\tilde{\Pi}_S^0$ , respectively. With  $\tilde{\Pi}_S^0$  invertible (which may be guaranteed by construction of  $\Pi_S^0$  as  $\text{rank} \Pi_S^0 = n_\xi + m$ ), solving for  $\Delta$  yields

$$\Delta = \left( \mathbf{H}_1(\mathcal{D}_{n_\xi+m}) - \tilde{\mathbf{H}}^{\text{LS}} \right) \left( \tilde{\Pi}_S^0 \right)^{-1}. \quad (19)$$

Finally, by substituting (19) in (18), we retrieve (17) with

$$\Gamma_2 = \left( \tilde{\Pi}_S^0 \right)^{-1} \Pi_S^0, \quad \Gamma_1 = \mathbf{H}_1(\mathcal{Y}_T) \Pi_S - \tilde{\mathbf{H}}^{\text{LS}} \Gamma_2. \quad (20)$$

Crucially, equation (17) of Proposition 2 offers a parameterization of all  $T$ -length disturbance trajectories consistent with the input and output data based on the first  $n_\xi + m$  of the  $T$  disturbances in the trajectory. For any choice of  $\mathcal{D}_{n_\xi+m}$  we obtain a consistent candidate  $\mathcal{D}_T$ .

**Remark 6** *Note that the number of free parameters  $p(n_\xi + m)$  in (17) is independent of the data length  $T$ . The intuition here is that the data  $\mathcal{D}_{n_\xi+m}, \mathcal{U}_{n_\xi+m}, \mathcal{Y}_{n_\xi+m}$ , implicitly determine the  $p(n_\xi + m)$  system parameters  $\Phi \in \mathbb{R}^{p \times n_\xi}, \Psi \in \mathbb{R}^{p \times m}$  of system (2) via (16). The remaining  $T - (n_\xi + m)$  disturbances in  $\mathcal{D}_T$  are then uniquely determined by the implied system parameters  $\Phi, \Psi$  and the remaining data in  $\mathcal{U}_T, \mathcal{Y}_T$ .*

#### B. Set of Consistent Disturbance Data

Given the disturbance bound in Assumption 2, we are not interested in all consistent disturbance trajectories  $\mathcal{D}_T$ , but only in those that are admissible, i.e.,  $\mathbf{d}_i^d \in \mathbb{D}$  for all  $i \in \mathbb{N}_1^T$  (see (7)). That is, the data trajectory  $\mathcal{D}_T$  must satisfy both

$$\mathbf{G}_d \mathbf{H}_1(\mathcal{D}_T) \leq \mathbf{1}_T^\top \otimes \mathbf{g}_d \quad (21)$$

and the consistency constraint (15). Note that the operation “ $\leq$ ” in (21) applies element-wise. The parameterization of the consistent disturbance data now allows to characterize the set

$\mathbb{D}^c$  of free parameters  $\mathcal{D}_{n_\xi+m}$  that give rise to disturbance trajectories satisfying the bound (21), namely

$$\mathbb{D}^c = \left\{ \mathcal{D}_{n_\xi+m} \mid \mathbf{G}_d \mathbf{H}_1(\mathcal{D}_{n_\xi+m}) \Gamma_2 \leq \mathbf{1}_T^\top \otimes \mathbf{g}_d - \mathbf{G}_d \Gamma_1 \right\}. \quad (22)$$

Note that (22) can be constructed purely from data.

Since the set of consistent disturbance data (22) is a polytopic set and inherits compactness from  $\mathbb{D}$  (see (21)), it can be described in terms of its vertices as  $\mathbb{D}^c = \text{conv} \left( \left\{ \mathcal{D}_{n_\xi+m, j} \right\}_{j=1}^{N_v} \right)$ , where  $N_v$  is the number of vertices. This representation can be used to derive the corresponding set of consistent system parameters

$$\mathbb{A} := \text{conv} \left( \left\{ \begin{bmatrix} \Phi_j & \Psi_j \end{bmatrix} \right\}_{j=1}^{N_v} \right) \quad (23)$$

by exploiting (16) and (17), with the matrix vertices  $\begin{bmatrix} \Phi_j & \Psi_j \end{bmatrix}$ .

### C. Incorporating Prior Model Knowledge

As the system matrices  $\Phi$ ,  $\Psi$  of (2) are related to the disturbance data  $\mathcal{D}_T$  via (16), we can incorporate prior model knowledge in the set of consistent disturbance data (e.g., knowledge on the structure and entries of  $\Phi$ ,  $\Psi$  like bounds or exact values). Consider the case where prior model knowledge for the system parameters  $\Phi$ ,  $\Psi$  is given in the following form with parameter matrices  $\mathbf{G}_{\mathbb{A},1}$ ,  $\mathbf{G}_{\mathbb{A},2}$ ,  $\mathbf{G}_{\mathbb{A},3}$  (cf. [27]):

$$\mathbf{G}_{\mathbb{A},1} \begin{bmatrix} \Phi & \Psi \end{bmatrix} \mathbf{G}_{\mathbb{A},2} \leq \mathbf{G}_{\mathbb{A},3}. \quad (24)$$

The set of system parameters that is defined via (24) is unbounded in general (i.e., bounds are not given for all system parameters) or might even have an empty interior (i.e., some system parameters might be exactly known, e.g., due to dynamic coupling).

In order to incorporate prior model knowledge of the form (24) into the set of consistent disturbance data (22), we first express (16) in terms of  $\mathcal{D}_{n_\xi+m}$ , i.e., the elements of the set of consistent disturbance data (22). By substituting (17) in (16), we retrieve

$$\begin{bmatrix} \Phi & \Psi \end{bmatrix} = \Gamma_1^\mathbb{A} + \mathbf{H}_1(\mathcal{D}_{n_\xi+m}) \Gamma_2^\mathbb{A}, \quad (25)$$

with the purely data-dependent parameters

$$\Gamma_1^\mathbb{A} = (\mathbf{H}_1(\mathcal{V}_T) - \Gamma_1) \mathbf{S}^\dagger, \quad \Gamma_2^\mathbb{A} = -\Gamma_2 \mathbf{S}^\dagger. \quad (26)$$

Now, using (25), we can translate (24) into constraints for the disturbance data  $\mathcal{D}_{n_\xi+m}$ , i.e.,

$$\mathbf{G}_{\mathbb{A},1} \mathbf{H}_1(\mathcal{D}_{n_\xi+m}) \Gamma_2^\mathbb{A} \mathbf{G}_{\mathbb{A},2} \leq \mathbf{G}_{\mathbb{A},3} - \mathbf{G}_{\mathbb{A},1} \Gamma_1^\mathbb{A} \mathbf{G}_{\mathbb{A},2} \quad (27)$$

which can be incorporated as additional linear constraints into (22). Note that the interior of (22) becomes empty if (24) has empty interior (the number of free parameters is reduced).

### D. Example

We conclude this section with an example that illustrates the findings regarding sets of consistent disturbance data (22).

Consider a system of the form (2) with  $T_p = 1$  and the matrices  $\Phi = \begin{bmatrix} 1 & 1 \end{bmatrix}$ ,  $\Psi = 0$ . From this system, a data trajectory  $\{\mathbf{u}_i^d\}_{i=0}^T$ ,  $\{\mathbf{y}_i^d\}_{i=0}^T$  of length  $T = 40$  is collected,

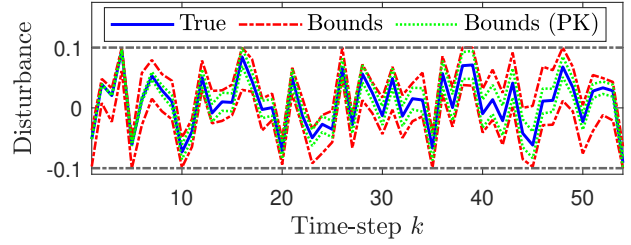


Fig. 1. Visualization of the consistency constraint on the disturbance data. The original disturbance bound is shown in black, while the true (unknown) disturbance data are given in blue. Bounds resulting from the set of consistent disturbance data (22) are depicted in red. The bounds depicted in green additionally include prior model knowledge.

satisfying Assumption 3, with inputs and disturbances randomly chosen within the bounds  $\|\mathbf{u}_k\|_\infty \leq 0.3$ ,  $\|\mathbf{d}_k\|_\infty \leq 0.1$  using an underlying uniform distribution. Using these data, the set of consistent disturbance data (22) is built (see Section III-B), which is illustrated in Fig. 1. It can be seen that the set of disturbance trajectories satisfying the consistency constraint (15) is remarkably smaller than the region that is defined by the original bound  $\|\mathbf{d}_k\|_\infty \leq 0.1$ . As also depicted in Fig. 1, the size of the set can be further reduced by considering prior model knowledge  $\Phi \begin{bmatrix} 0 & 1 \end{bmatrix}^\top = 1$ ,  $\Psi = 0$ .

In the following section, Proposition 2 and (22) are used to derive data-driven predictors based on the extended fundamental lemma (Lemma 2). Samples of consistent disturbance data as well as samples of potential future disturbances allow for deterministic reformulation of the chance constraint (13c), yielding a tractable stochastic DPC scheme based on (13).

## IV. SAMPLING-BASED STOCHASTIC DPC

In this section, we elaborate on the design steps of the proposed predictive controller based on OCP (13), using the concept of sampling-based chance constraints approximation.

As discussed in Section II-C, we render OCP (13) tractable by replacing the unknown disturbance data  $\mathcal{D}_T$  with samples from the set of consistent disturbance data (22), and the future disturbances  $\mathbf{d}_{f,k}$  with samples from the disturbance set (7). This leads to a deterministic approximation of OCP (13) where the chance constraint (13c) is replaced by an inner-approximation constructed from samples. Samples are drawn from the probability distribution given in Assumption 2.

### A. Data-driven Sample-based Predictors

We next derive predictors for future outputs, inputs, and terminal extended state based on the available system data and samples of the past disturbance data and future disturbances as follows. From Lemma 2, we get that there exists an  $\alpha = \alpha^{(i)}$  that satisfies (13b) for every sampled disturbance data trajectory  $\mathcal{D}_T^{(i)}$  and future disturbances  $\mathbf{d}_{f,k}^{(i)}$ , with fixed initial condition  $\xi_k$  and sequence of correction inputs  $\mathbf{v}_{f,k}$ . Since the data are now certain, an exact data-driven output predictor follows from

$$\alpha^{(i)} = \begin{bmatrix} \mathbf{H}_1(\mathcal{X}_{T-T_i+1}) \\ \mathbf{H}_{T_i}(\mathcal{V}_T) \\ \mathbf{H}_{T_i}(\mathcal{D}_T^{(i)}) \end{bmatrix}^\dagger \begin{bmatrix} \xi_k \\ \mathbf{v}_{f,k} \\ \mathbf{d}_{f,k}^{(i)} \end{bmatrix}, \quad (28)$$

in the form of

$$\mathbf{y}_{f,k}^{(i)} = \mathbf{M}_y^{(i)} \begin{bmatrix} \boldsymbol{\xi}_k \\ \mathbf{v}_{f,k} \end{bmatrix} + \mathbf{m}_y^{(i)}, \quad (29)$$

with  $\mathbf{M}_y^{(i)}$ ,  $\mathbf{m}_y^{(i)}$  defined based on  $\boldsymbol{\alpha}^{(i)}$  as in Appendix II. Analogously, input trajectories including the state feedback  $\mathbf{u}_k = \mathbf{K}\boldsymbol{\xi}_k + \mathbf{v}_k$  (12) may directly be computed as

$$\mathbf{u}_{f,k}^{(i)} = \mathbf{M}_u^{(i)} \begin{bmatrix} \boldsymbol{\xi}_k \\ \mathbf{v}_{f,k} \end{bmatrix} + \mathbf{m}_u^{(i)}, \quad (30)$$

and the sampled terminal extended state follows from

$$\boldsymbol{\xi}_{T|k}^{(i)} = \mathbf{M}_\xi^{(i)} \begin{bmatrix} \boldsymbol{\xi}_k \\ \mathbf{v}_{f,k} \end{bmatrix} + \mathbf{m}_\xi^{(i)}, \quad (31)$$

with  $\mathbf{M}_u^{(i)}$ ,  $\mathbf{m}_u^{(i)}$ ,  $\mathbf{M}_\xi^{(i)}$ ,  $\mathbf{m}_\xi^{(i)}$  defined in Appendix II.

Given an initial extended state  $\boldsymbol{\xi}_k$  and a sequence of correction inputs  $\mathbf{v}_{f,k}$ , the predictors (29), (30) exactly compute the resulting input-output trajectory for the sampled uncertainty realization in a purely data-based manner. We remark that the multi-step predictors (29)–(31) coincide with the predictors commonly used in SPC [19], and that DPC and SPC yield the same (certainty-equivalence) predictor when using a consistent disturbance sample  $\mathcal{D}_T^{(i)}$  in (28) [20]. Consequently, the predictors (29)–(31) allow to reformulate the constraints (13c)–(13e) and the cost function (13a) in terms of the measured extended state  $\boldsymbol{\xi}_k$  and the input sequence  $\mathbf{v}_{f,k}$ , i.e., the minimal amount of (deterministic) optimization variables.

## B. Constraint Sampling

In order to render the OCP (13) tractable, the chance constraint (8a) needs to be reformulated into a deterministic expression. Thus, in the following, we describe how to reformulate the constraints (13c)–(13e) in terms of the previously derived data-driven predictors (29)–(31), and how to deterministically approximate the chance constraint (13c) via sampling of the uncertainty. In our setting, the extended state  $\boldsymbol{\xi}_k$  and the sequence of future correction inputs  $\mathbf{v}_{f,k}$  from (13) will act as the deterministic decision variables for the approximation, whereas the disturbance data trajectory  $\mathcal{D}_T$  and future disturbances  $\mathbf{d}_{f,k}$  take the role of the uncertainty.

Let us define the set of deterministic decision variables  $\text{col}(\boldsymbol{\xi}_k, \mathbf{v}_{f,k})$  for which the joint chance constraint (13c) for the predicted outputs  $\mathbf{y}_{l|k}$ ,  $l \in \mathbb{N}_0^{T_l-1}$ , from the OCP (13) is satisfied with a probability of at least  $1 - \varepsilon$  as

$$\mathbb{Y}_l^P = \left\{ \begin{bmatrix} \boldsymbol{\xi}_k \\ \mathbf{v}_{f,k} \end{bmatrix} \mid \Pr[\mathbf{G}_y \mathbf{y}_{l|k} \leq \mathbf{g}_y] \geq 1 - \varepsilon \right\}. \quad (32)$$

Sets of the form (32) are commonly referred to as  $\varepsilon$ -chance constraint set ( $\varepsilon$ -CCS) [16]. Note that  $\mathbf{y}_{l|k}$  is related to  $\text{col}(\boldsymbol{\xi}_k, \mathbf{v}_{f,k})$  via (13b). The goal of the offline sampling-based approach is to determine a deterministic inner-approximation  $\mathbb{Y}_l^S$  of the  $\varepsilon$ -CCS (32) by using  $N_s$  iid samples  $\mathbf{w}^{(i)} := \{\mathcal{D}_T^{(i)}, \mathbf{d}_{f,k}^{(i)}\}$ ,  $i \in \mathbb{N}_1^{N_s}$  of the uncertainty. More formally, the inner-approximation satisfies  $\Pr[\mathbb{Y}_l^S \subseteq \mathbb{Y}_l^P] \geq 1 - \varepsilon^c$  with a pre-defined level of confidence  $\varepsilon^c$ .

Given an uncertainty sample  $\mathbf{w}^{(i)}$  and the predictor (29), the sampled set corresponding to the output  $\varepsilon$ -CCS (32) reads

$$\tilde{\mathbb{Y}}_l^S(\mathbf{w}^{(i)}) = \left\{ \begin{bmatrix} \boldsymbol{\xi}_k \\ \mathbf{v}_{f,k} \end{bmatrix} \mid \mathbf{G}_{y,l}^{(i)} \begin{bmatrix} \boldsymbol{\xi}_k \\ \mathbf{v}_{f,k} \end{bmatrix} \leq \mathbf{g}_{y,l}^{(i)} \right\}, \quad (33)$$

with the sampled constraint parameters

$$\mathbf{G}_{y,l}^{(i)} := \mathbf{G}_y \left[ \mathbf{M}_y^{(i)} \right]_{[lp+1:(l+1)p]}, \quad (34a)$$

$$\mathbf{g}_{y,l}^{(i)} := \mathbf{g}_y - \mathbf{G}_y \left[ \mathbf{m}_y^{(i)} \right]_{[lp+1:(l+1)p]}. \quad (34b)$$

In Appendix III, we discuss two popular approaches to the sampling-based approximation of  $\varepsilon$ -CCSs, namely the direct sampling-based approximation and the probabilistic scaling approach. Both approaches make use of the sampled set as in (33) that corresponds to the  $\varepsilon$ -CCS as in (32). Using the definition of the sampled set (33) and  $N_s$  samples of  $\mathbf{w}^{(i)}$ , we thus derive a deterministic constraint set  $\mathbb{Y}_l^S$  that inner-approximates  $\mathbb{Y}_l^P$  with a pre-defined level of confidence  $\varepsilon^c$  supported by either sampling approach presented in Appendix III.

1) *Direct Approximation*: Draw  $N_s \geq N_{LT}(\varepsilon, \varepsilon^c, n_\xi + m(l+1), n_{c,y})$  uncertainty samples  $\mathbf{w}^{(i)}$ , where  $n_{c,y}$  is the number of output constraints in (8a). By Proposition 4, the set  $\mathbb{Y}_l^S := \bigcap_{i=0}^{N_s} \tilde{\mathbb{Y}}_l^S(\mathbf{w}^{(i)})$  satisfies  $\Pr[\mathbb{Y}_l^S \subseteq \mathbb{Y}_l^P] \geq 1 - \varepsilon^c$ , thus retrieving a valid inner-approximation of (13c).

2) *Probabilistic Scaling*: Draw  $\tilde{N}_s$  “design” uncertainty samples  $\mathbf{w}^{(i)}$  and construct a polytopic candidate simple approximating set (SAS)  $\mathbb{Y}_l^S(\sigma) := \{\mathbf{c}\} \oplus \sigma(\mathbb{Y}_l^{\text{SAS}} \ominus \{\mathbf{c}\})$ , where  $\mathbb{Y}_l^{\text{SAS}} := \bigcap_{i=0}^{\tilde{N}_s} \tilde{\mathbb{Y}}_l^S(\mathbf{w}^{(i)})$  and  $\mathbf{c}$  is a center (e.g., Chebyshev or geometric center) of  $\mathbb{Y}_l^{\text{SAS}}$ . Draw  $N_s \geq N_{PS}(\varepsilon, \varepsilon^c)$  uncertainty samples and apply Proposition 5 to retrieve the set  $\mathbb{Y}_l^S(\sigma^*)$  that satisfies  $\Pr[\mathbb{Y}_l^S(\sigma^*) \subseteq \mathbb{Y}_l^P] \geq 1 - \varepsilon^c$ , thus retrieving a valid inner-approximation of (13c).

Due to the state feedback in (12), uncertainty is also introduced into the predicted inputs  $\mathbf{u}_{l|k}$  for  $l \in \mathbb{N}_1^{T_l-1}$ . In order to accommodate this uncertainty, we approximate the hard input constraints (13d) in the prediction horizon analogously to the chance constraints by defining a new risk parameter  $\varepsilon_u$  and confidence level  $\varepsilon_u^c$ , yielding polytopic constraint sets  $\tilde{\mathbb{U}}_l$  for  $l \in \mathbb{N}_0^{T_l-1}$ , where  $\tilde{\mathbb{U}}_0 = \mathbb{U}$  for the input that is actually applied. Similarly, the terminal constraint set (13e) is approximated based on the terminal state predictor (31) and the definition of a new risk parameter  $\varepsilon_\xi$  and confidence level  $\varepsilon_\xi^c$ , yielding the sampled terminal constraint set  $\tilde{\mathbb{X}}_{T_l}$ . By use of the predictors for input (30) and terminal state (31), these constraint sets are transformed into constraints on the extended state  $\boldsymbol{\xi}_k$  and correction inputs  $\mathbf{v}_{f,k}$ . In order to conclude the constraint sampling, we define the aggregate constraint set

$$\mathbb{C} = \left\{ \begin{bmatrix} \boldsymbol{\xi}_k \\ \mathbf{v}_{f,k} \end{bmatrix} \mid \mathbf{G}_{\text{OCP}} \begin{bmatrix} \boldsymbol{\xi}_k \\ \mathbf{v}_{f,k} \end{bmatrix} \leq \mathbf{g}_{\text{OCP}} \right\} \quad (35)$$

as the intersection of the sampled input, output, and terminal constraints  $\tilde{\mathbb{U}}_l$ ,  $\tilde{\mathbb{Y}}_l$ ,  $\tilde{\mathbb{X}}_{T_l}$  for all predicted steps  $l \in \mathbb{N}_0^{T_l-1}$ , with corresponding constraint parameters  $\mathbf{G}_{\text{OCP}}$ ,  $\mathbf{g}_{\text{OCP}}$ .

## C. Reformulation of the Cost Function

Besides the constraints, also the cost function (9) needs to be deterministically approximated. We do so by exploiting sample

average approximation [29] and the data-driven predictors (29)–(31): For an input prediction  $\mathbf{u}_{f,k}^{(i)}$ , output prediction  $\mathbf{y}_{f,k}^{(i)}$ , and terminal state prediction  $\boldsymbol{\xi}_{T_f|k}^{(i)}$  resulting from an uncertainty sample  $\mathbf{w}^{(i)}$ , denote the sampled cost as

$$J_{T_f}^{(i)} = \left\| \mathbf{y}_{f,k}^{(i)} \right\|_{\tilde{\mathbf{Q}}}^2 + \left\| \mathbf{u}_{f,k}^{(i)} \right\|_{\tilde{\mathbf{R}}}^2 + \left\| \boldsymbol{\xi}_{T_f|k}^{(i)} \right\|_{\mathbf{P}}^2, \quad (36)$$

where  $\tilde{\mathbf{Q}} := \mathbf{I}_{T_f} \otimes \mathbf{Q}$  and  $\tilde{\mathbf{R}} := \mathbf{I}_{T_f} \otimes \mathbf{R}$ . By expressing  $J_{T_f}^{(i)}$  in terms of initial extended state  $\boldsymbol{\xi}_k$  and predicted correction inputs  $\mathbf{v}_{f,k}$  via (29)–(31), we retrieve

$$J_{T_f}^{(i)} = \left\| \begin{bmatrix} \boldsymbol{\xi}_k \\ \mathbf{v}_{0|k} \end{bmatrix} \right\|_{\mathbf{Q}_{\text{OCP}}^{(i)}}^2 + 2\mathbf{q}_{\text{OCP}}^{(i)\top} \begin{bmatrix} \boldsymbol{\xi}_k \\ \mathbf{v}_{f,k} \end{bmatrix} + c^{(i)} \quad (37)$$

with the sampled cost parameters

$$\begin{aligned} \mathbf{Q}_{\text{OCP}}^{(i)} &:= \mathbf{M}_y^{(i)\top} \tilde{\mathbf{Q}} \mathbf{M}_y^{(i)} + \mathbf{M}_u^{(i)\top} \tilde{\mathbf{R}} \mathbf{M}_u^{(i)} + \mathbf{M}_\xi^{(i)\top} \mathbf{P} \mathbf{M}_\xi^{(i)}, \\ \mathbf{q}_{\text{OCP}}^{(i)} &:= \mathbf{M}_y^{(i)\top} \tilde{\mathbf{Q}} \mathbf{m}_y^{(i)} + \mathbf{M}_u^{(i)\top} \tilde{\mathbf{R}} \mathbf{m}_u^{(i)} + \mathbf{M}_\xi^{(i)\top} \mathbf{P} \mathbf{m}_\xi^{(i)}, \\ c^{(i)} &:= \mathbf{m}_y^{(i)\top} \tilde{\mathbf{Q}} \mathbf{m}_y^{(i)} + \mathbf{m}_u^{(i)\top} \tilde{\mathbf{R}} \mathbf{m}_u^{(i)} + \mathbf{m}_\xi^{(i)\top} \mathbf{P} \mathbf{m}_\xi^{(i)}. \end{aligned}$$

Based on  $N_s^{\text{avg}}$  uncertainty samples  $\mathbf{w}^{(i)}$ , the sample-average cost function that approximates (9) to a desired level of accuracy reads as

$$J_{T_f}(\boldsymbol{\xi}_k, \mathbf{v}_{f,k}) = \left\| \begin{bmatrix} \boldsymbol{\xi}_k \\ \mathbf{v}_{0|k} \end{bmatrix} \right\|_{\mathbf{Q}_{\text{OCP}}}^2 + 2\mathbf{q}_{\text{OCP}}^\top \begin{bmatrix} \boldsymbol{\xi}_k \\ \mathbf{v}_{f,k} \end{bmatrix} + c, \quad (39)$$

where  $c := \frac{1}{N_s^{\text{avg}}} \sum_{i=1}^{N_s^{\text{avg}}} c^{(i)}$  is a constant that can be neglected in the optimization, and

$$\mathbf{Q}_{\text{OCP}} := \frac{1}{N_s^{\text{avg}}} \sum_{i=1}^{N_s^{\text{avg}}} \mathbf{Q}_{\text{OCP}}^{(i)}, \quad \mathbf{q}_{\text{OCP}} := \frac{1}{N_s^{\text{avg}}} \sum_{i=1}^{N_s^{\text{avg}}} \mathbf{q}_{\text{OCP}}^{(i)}. \quad (40)$$

In the following, we assume that (9) and (39) coincide. Note that, instead of sample-average approximation, the expected value for the cost parameters in (39) can also be approximated to the desired level of accuracy using an appropriate numerical integration scheme [15].

#### D. Control Algorithm

Based on the previously derived constraints (35), (45) and cost function (39), we define the OCP that is solved at each time-step  $k$  as

$$J_{T_f}^*(\boldsymbol{\xi}_k) = \min_{\mathbf{v}_{f,k}} J_{T_f}(\boldsymbol{\xi}_k, \mathbf{v}_{f,k}) \quad (41a)$$

$$\text{s.t. } \begin{bmatrix} \boldsymbol{\xi}_k \\ \mathbf{v}_{f,k} \end{bmatrix} \in \mathbb{C} \cap \mathbb{C}_{\mathbf{R}}, \quad (41b)$$

with suitable  $\mathbb{C}_{\mathbf{R}}$  that guarantees recursive feasibility via a robust constraint on the first predicted step. How to construct  $\mathbb{C}_{\mathbf{R}}$  using (35) is discussed in Section V-A. We remark that a solution to (41) can only exist if  $\mathbb{C} \cap \mathbb{C}_{\mathbf{R}}$  is non-empty. For that, it is necessary that the bounds in Assumptions 2 are suitably tight, as large disturbance bounds likely lead to an empty intersection  $\mathbb{C}$  of the sampled constraint sets. The implicit control law associated with OCP (41) reads

$$\boldsymbol{\kappa}(\boldsymbol{\xi}_k) := \mathbf{u}_k^* = \mathbf{K} \boldsymbol{\xi}_k + \mathbf{v}_{0|k}^* \quad (42)$$

where  $\mathbf{v}_{0|k}^* = \begin{bmatrix} \mathbf{v}_{f,k}^* \end{bmatrix}_{[1:m]}$  is the first input of the optimal input vector  $\mathbf{v}_{f,k}^*$ . The overall algorithm of the proposed controller is summarized in Algorithm 1, split into an offline and online phase.

---

#### Algorithm 1 Sampling-based Stochastic DPC

---

##### Offline Phase:

- 1: Retrieve an input-output data trajectory from system (2) that satisfies Assumption 3.
- 2: Compute the set of consistent disturbance data (22).
- 3: Determine suitable  $\mathbf{K}$ ,  $\mathbf{P}$ , and  $\mathbb{X}_{T_f}$  (see Appendix I).
- 4: Compute constraint set  $\mathbb{C}$  (35) from (consistent) disturbance samples.
- 5: Compute the first-step constraint  $\mathbb{C}_{\mathbf{R}}$  (see Section V-A) and the intersection  $\mathbb{C} \cap \mathbb{C}_{\mathbf{R}}$ .
- 6: Determine the weights of the cost function (39).

##### Online Phase:

- 7: **for**  $k \geq 0$  **do**
  - 8:   Construct the current extended state  $\boldsymbol{\xi}_k$  from the most recent past  $T_p$  input-output measurements.
  - 9:   Solve the OCP (41) to retrieve  $\mathbf{v}_{0|k}^*$
  - 10:   Apply the input  $\mathbf{u}_k = \mathbf{v}_{0|k}^* + \mathbf{K} \boldsymbol{\xi}_k$  to the system.
  - 11: **end for**
- 

#### E. Discussion

The proposed controller is lightweight as all heavy computations are performed in the offline phase, leading to a dense quadratic program in the online phase for which efficient solvers exist. To further reduce the online computational load, redundant constraints should be removed from the final constraint set (41b). Redundancy removal algorithms are described in [15], [30].

The data-driven predictors (29)–(31) require samples of potential future disturbances and of consistent disturbance data. From Assumption 2, the distribution and the polytopic support set of the disturbance are given. Similarly for the unknown disturbance data, we retrieve a polytopic support set (22) considering consistency with the given input-output data and system class (see Section III). Thus, to generate disturbance samples, we need to sample from a distribution that is truncated over a polytopic set. One option is to use rejection sampling [31], however, its efficiency depends on the size of the polytopic support set. For uniform distributions, efficient sampling methods exist [32].

## V. CLOSED-LOOP PROPERTIES

In the following, we present properties of the closed-loop system that results from application of the proposed controller (42) to system (2), or, equivalently, (5):

$$\boldsymbol{\xi}_{k+1} = \tilde{\mathbf{A}} \boldsymbol{\xi}_k + \tilde{\mathbf{B}} \boldsymbol{\kappa}(\boldsymbol{\xi}_k) + \tilde{\mathbf{E}} \mathbf{d}_k, \quad (43a)$$

$$\mathbf{y}_k = \Phi \boldsymbol{\xi}_k + \Psi \boldsymbol{\kappa}(\boldsymbol{\xi}_k) + \mathbf{d}_k. \quad (43b)$$

In order to guarantee stability, we assume the existence of a suitable stabilizing feedback-gain  $\mathbf{K}$  (see (12)), weighting

matrix  $\mathbf{P}$  for the terminal cost (see (9)), and RPI terminal constraint  $\mathbb{X}_{T_f}$  (see (13e)), based on an outer-bounding polytopic set (23) for the system parameters in (2). This is summarized in Assumption 5 and is common in robust and stochastic predictive control [15], [33], [34]. Existing literature can be used to determine these ingredients from the available data [8], [25], [35], which is presented in Appendix I for our setting.

**Assumption 5 (Stabilizing Ingredients)** *Let  $\mathbf{R}, \mathbf{Q} \succ \mathbf{0}$  be the weighting matrices from (9) and let  $\tilde{\mathbf{A}} := \text{conv}(\{[\tilde{\mathbf{A}}_j \ \tilde{\mathbf{B}}_j]\}_{j=1}^{N_v})$ ,  $\tilde{\mathbf{A}}_j := \text{col}(\tilde{\mathbf{A}}, \tilde{\Phi}_j)$ ,  $\tilde{\mathbf{B}}_j := \text{col}(\tilde{\mathbf{B}}, \tilde{\Psi}_j)$  be constructed by using (6) and the vertices  $[\tilde{\Phi}_j \ \tilde{\Psi}_j]$ ,  $j \in \mathbb{N}_1^{N_v}$  from (23). There exist a feedback gain  $\mathbf{K}$  and weighting matrix  $\mathbf{P} = \mathbf{P}^\top \succ \mathbf{0}$  such that for all  $j \in \mathbb{N}_1^{N_v}$*

(a)  $\tilde{\mathbf{A}}_{\text{cl},j} := \tilde{\mathbf{A}}_j + \mathbf{K}\tilde{\mathbf{B}}_j$  is Schur stable, and  
(b)  $\tilde{\mathbf{A}}_{\text{cl},j}^\top \mathbf{P} \tilde{\mathbf{A}}_{\text{cl},j} - \mathbf{P} + \mathbf{K}^\top \mathbf{R} \mathbf{K} + \tilde{\mathbf{A}}_{\text{cl},j}^\top \tilde{\mathbf{E}} \mathbf{Q} \tilde{\mathbf{E}}^\top \tilde{\mathbf{A}}_{\text{cl},j} \prec \mathbf{0}$ ,  
with  $\tilde{\mathbf{E}} = \text{col}(\mathbf{0}, \mathbf{I}_p)$ . Furthermore, the terminal set  $\mathbb{X}_{T_f} = \{\xi \in \mathbb{R}^{n_\xi} \mid \tilde{\mathbf{G}}_\xi \xi \leq \tilde{\mathbf{g}}_\xi\}$  for system (2) is robustly invariant under the control law  $\mathbf{u}_k = \mathbf{K}\xi_k$ , and the constraints (8) are satisfied  $\forall \xi_k \in \mathbb{X}_{T_f}$ .

### A. Recursive Feasibility

In order to render OCP (41) recursively feasible, we construct an additional constraint  $\mathbb{C}_R$  on the first predicted step, following ideas from [15]. Let  $\mathbb{C}_{T_f}$  denote the set of feasible initial extended state and first input, computed by projection of (35):

$$\mathbb{C}_{T_f} := \left\{ \left[ \begin{array}{c} \xi_k \\ \mathbf{v}_{0|k} \end{array} \right] \mid \begin{array}{l} \exists \mathbf{v}_{1|k}, \dots, \mathbf{v}_{T_f-1|k} \in \mathbb{R}^m : \\ \text{col}(\xi_k, \mathbf{v}_{f,k}) \in \mathbb{C} \end{array} \right\}. \quad (44)$$

Based on the matrix vertices  $\tilde{\mathbf{A}}_{\text{cl},j}$ ,  $j \in \mathbb{N}_1^{N_v}$  as defined in Assumption 5(a) and the disturbance bound  $\mathbb{D}$  from (7), we determine a (maximal) robust control invariant set for system (5) with  $\text{col}(\xi_k, \mathbf{v}_{0|k}) \in \mathbb{C}_{T_f}$  of the form  $\mathbb{C}_\xi^\infty := \{\xi \in \mathbb{R}^{n_\xi} \mid \mathbf{G}_\xi^\infty \xi \leq \mathbf{g}_\xi^\infty\}$  [35]. At last, we construct the first-step constraint set

$$\mathbb{C}_R := \left\{ \left[ \begin{array}{c} \xi_k \\ \mathbf{v}_{f,k} \end{array} \right] \mid \forall \mathbf{d} \in \mathbb{D}, j \in \mathbb{N}_1^{N_v} : \right. \\ \left. \tilde{\mathbf{A}}_{\text{cl},j} \xi_k + \tilde{\mathbf{B}}_j \mathbf{v}_{0|k} + \tilde{\mathbf{E}} \mathbf{d} \in \mathbb{C}_\xi^\infty \right\}. \quad (45)$$

Now, since the constraint set  $\mathbb{C} \cap \mathbb{C}_R$  is RPI for the closed-loop dynamics (43a), OCP (41) is recursively feasible.

**Theorem 1 (Recursive Feasibility)** *Let  $\mathbb{F}(\xi_k)$  be the set of all feasible input sequences for a given extended state  $\xi_k$ , i.e.,*

$$\mathbb{F}(\xi_k) = \{\mathbf{v}_{f,k} \mid \text{col}(\xi_k, \mathbf{v}_{f,k}) \in \mathbb{C} \cap \mathbb{C}_R\}. \quad (46)$$

*For every realization of  $\mathbf{d}_k \in \mathbb{D}$ , it holds that  $\mathbb{F}(\xi_k) \neq \emptyset \implies \mathbb{F}(\xi_{k+1}) \neq \emptyset$  under the proposed control law (42).*

*Proof:* By robustness of the first-step constraint (45),  $\text{col}(\xi_k, \mathbf{v}_{f,k}) \in \mathbb{C}_R$  implies  $\xi_{k+1} \in \mathbb{C}_\xi^\infty$ . By construction, it holds that  $\mathbb{C}_\xi^\infty \subset \{\xi \mid \mathbb{F}(\xi) \neq \emptyset\}$ , which proves the claim. ■

From recursive feasibility follows constraint satisfaction.

**Corollary 1 (Closed-loop Constraint Satisfaction)** *Let  $\xi_0 \in \mathbb{C}_\xi^\infty$ . The closed-loop system (43b) satisfies the specified*

*output chance constraints (8a) with confidence  $\varepsilon^c$  and the hard input constraints (8b) for all time-steps  $k \geq 0$ .*

*Proof:* With  $\xi_0 \in \mathbb{C}_\xi^\infty$ , a feasible pair  $\text{col}(\xi_0, \mathbf{v}_{f,0}) \in \mathbb{C}$  exists by design. Closed-loop input constraint satisfaction follows from Theorem 1 and the constraint  $\mathbf{v}_{0|k} + \mathbf{K}\xi_k \in \tilde{\mathbb{U}}_0 = \mathbb{U}$ , which is included in the constraint set  $\mathbb{C}$ . Furthermore, it holds that  $\mathbb{C} \subseteq \tilde{\mathbb{Y}}_0$ , and  $\tilde{\mathbb{Y}}_0 \subseteq \mathbb{Y}_0^P$  with confidence  $1 - \varepsilon^c$  by design (see Section IV-B). Thus, the chance constraint  $\Pr[\mathbf{G}_y \mathbf{y}_{0|k} \leq \mathbf{g}_y] \geq 1 - \varepsilon$  is satisfied with confidence  $1 - \varepsilon^c$  for all feasible  $\text{col}(\xi_k, \mathbf{v}_{f,k}) \in \mathbb{C}$ ,  $k \geq 0$ , which is sufficient for satisfaction of chance constraint (8a) in closed-loop. ■

### B. Robust Asymptotic Stability in Expectation

We now analyze convergence properties of the closed-loop system under the proposed controller. Literature on stochastic predictive control often provides mean-square stability guarantees via average asymptotic cost bounds [8], [17], [34], [36]. In contrast, we consider a stronger notion of stability in this work, namely robust asymptotic stability in expectation (RASiE).

**Definition 3 (RASiE [21])** *Let  $\mathbb{C}_\xi^\infty$  be a closed RPI set for the stochastic system (43a) with the origin in its interior, and let  $\xi_k$  denote the solution to (43a) at time  $k \in \mathbb{N}_0$  for given initial condition  $\xi_0$  and disturbance trajectory  $\{\mathbf{d}_0, \dots, \mathbf{d}_k\}$ . The origin of system (43a) is robustly asymptotically stable in expectation on  $\mathbb{C}_\xi^\infty$  if there exist functions  $\beta \in \mathcal{KL}$  and  $\varrho \in \mathcal{K}$  such that*

$$\mathbb{E}[\|\xi_k\|] \leq \beta(\|\xi_0\|, k) + \varrho(\text{tr}(\Sigma)) \quad (47)$$

*for all  $k \in \mathbb{N}_0$  and  $\xi_0 \in \mathbb{C}_\xi^\infty$ , with covariance  $\Sigma := \mathbb{E}[\mathbf{d}\mathbf{d}^\top]$ .*

RASiE not only provides a uniform bound on the expected value of the norm of the closed-loop state, but it also gives insight into the dependency of this bound on the disturbance covariance, and it ensures that the effect of the initial condition  $\xi_0$  on this bound asymptotically decays towards zero [21]. In contrast to input-to-state stability (ISS) [37], RASiE considers the expected value of the norm of the closed-loop state and the covariance matrix of the disturbance. RASiE can be established with the help of a stochastic ISS Lyapunov function, as stated in the following proposition.

### Proposition 3 (Stochastic ISS Lyapunov Function [21])

*The origin of the closed-loop system (43a) is RASiE on the RPI set  $\mathbb{C}_\xi^\infty$  if there exists a function  $V : \mathbb{C}_\xi^\infty \rightarrow \mathbb{R}_{\geq 0}$  and functions  $\varrho_1, \varrho_2, \varrho_3 \in \mathcal{K}_\infty$ ,  $\varrho_4, \varrho_5 \in \mathcal{K}$  such that*

$$\varrho_1(\|\xi_k\|) \leq V(\xi_k) \leq \varrho_2(\|\xi_k\|) + \varrho_4(\text{tr}(\Sigma)), \quad (48a)$$

$$\mathbb{E}[V(\xi_{k+1})] - V(\xi_k) \leq -\varrho_3(\|\xi_k\|) + \varrho_5(\text{tr}(\Sigma)) \quad (48b)$$

*holds for all  $\xi_k \in \mathbb{C}_\xi^\infty$ . The function  $V$  is then called a stochastic ISS Lyapunov function.*

Commonly, stability proofs for predictive controllers rely on the availability of a feasible candidate solution  $\tilde{\mathbf{v}}_{f,k+1} \in \mathbb{F}(\xi_{k+1})$  (see (46)) to show descent in the Lyapunov function similar to (48b). Although we have shown recursive feasibility

in Theorem 1, guaranteeing feasibility of the candidate solution at all time-steps is in general impossible for sampling-based predictive controllers, as has been pointed out in [15]. Nonetheless, stability of the closed-loop system can still be guaranteed if the probability of infeasibility of the candidate solution is sufficiently low [15], [17]. For our setting, we define the candidate solution as follows (cf. [17], [38]).

**Definition 4 (Candidate Solution)** *Given the OCP (41) and a feasible solution  $\mathbf{v}_{f,k}^*$  at time-step  $k$ , we define the candidate solution for time-step  $k+1$  as  $\tilde{\mathbf{v}}_{f,k+1} := \text{col}(\tilde{\mathbf{v}}_{0|k+1}, \dots, \tilde{\mathbf{v}}_{T_f-1|k+1})$  with*

$$\tilde{\mathbf{v}}_{l|k+1} := \begin{cases} \mathbf{v}_{l+1|k}^* + \mathbf{K} \tilde{\mathbf{A}}_{\text{cl}}^l \tilde{\mathbf{E}} \mathbf{d}_k, & l \in \mathbb{N}_0^{T_f-2} \\ \mathbf{K} \tilde{\mathbf{A}}_{\text{cl}}^l \tilde{\mathbf{E}} \mathbf{d}_k & l = T_f - 1 \end{cases} \quad (49)$$

If the candidate solution is infeasible, we make use of the following assumption to bound the cost increase (cf. [17]).

**Assumption 6 (Bounded Optimal Cost Function)** *Let  $J_{T_f}^*(\boldsymbol{\xi}_k)$  be the optimal cost function of the OCP (41). There exist  $\mathbf{P}_1 \succ \mathbf{0}$ ,  $\mathbf{P}_u \succ \mathbf{0}$ ,  $c \in \mathbb{R}$  such that  $\|\boldsymbol{\xi}_k\|_{\mathbf{P}_1}^2 \leq J_{T_f}^*(\boldsymbol{\xi}_k) - c \leq \|\boldsymbol{\xi}_k\|_{\mathbf{P}_u}^2$  holds for all  $\boldsymbol{\xi}_k \in \mathbb{C}_\xi^\infty$ .*

The matrix  $\mathbf{P}_1$  can be chosen according to the unconstrained infinite horizon cost, while  $\mathbf{P}_u$  can be determined using the vertices of the set of feasible initial extended states  $\mathbb{C}_\xi^\infty$  [15].

We now present our main result, namely RASiE of the closed-loop system (43a) under the proposed control law (42). We prove the theorem by construction of a stochastic ISS Lyapunov function that is admitted by the closed-loop dynamics (43a) on  $\mathbb{C}_\xi^\infty$ , which is sufficient for RASiE (see Proposition 3). We do so by 1) bounding the expected increase of the optimal cost  $J_{T_f}^*(\boldsymbol{\xi}_k)$  similar to [17] but in our input-output setting, and 2) constructing a stochastic ISS Lyapunov function using the optimal cost  $J_{T_f}^*(\boldsymbol{\xi}_k)$  and an input-output-to-state stability (IOSS) Lyapunov function similar to [28]. Note that, since system (5) is detectable, there exists an IOSS Lyapunov function of the form  $W(\boldsymbol{\xi}_k) = \|\boldsymbol{\xi}_k\|_{\mathbf{P}_W}^2$ , satisfying

$$\begin{aligned} W(\boldsymbol{\xi}_{k+1}) - W(\boldsymbol{\xi}_k) \\ \leq -\frac{1}{2} \|\boldsymbol{\xi}_k\|^2 + c_u \|\mathbf{u}_k\|^2 + c_y \|\mathbf{y}_k\|^2 + c_d \|\mathbf{d}_k\|^2, \end{aligned} \quad (50)$$

with suitable parameters  $\mathbf{P}_W \succ \mathbf{0}$ ,  $c_u, c_y, c_d > 0$  that can be determined using  $\tilde{\mathbf{A}}$  from Assumption 5, cf. [28], [39].

**Theorem 2 (RASiE of the Closed-loop)** *Let  $\varepsilon_f \in [0, 1)$  be an upper bound of the probability that the candidate solution (49) is not feasible. The origin of system (43a) is robustly asymptotically stable in expectation on  $\mathbb{C}_\xi^\infty$  if  $\mathbf{Q}_S \succ \mathbf{0}$  holds, with*

$$\mathbf{Q}_S := \begin{bmatrix} \frac{c_S}{2} \mathbf{I}_{n_\xi} & \mathbf{0} \\ \mathbf{0} & \mathbf{R}_S \end{bmatrix} - \frac{\varepsilon_f}{1 - \varepsilon_f} \begin{bmatrix} \tilde{\mathbf{A}}^\top \mathbf{P}_u \tilde{\mathbf{A}} - \mathbf{P}_1 & \tilde{\mathbf{A}}^\top \mathbf{P}_u \tilde{\mathbf{B}} \\ \tilde{\mathbf{B}}^\top \mathbf{P}_u \tilde{\mathbf{A}} & \tilde{\mathbf{B}}^\top \mathbf{P}_u \tilde{\mathbf{B}} \end{bmatrix}, \quad (51)$$

$\mathbf{R}_S := \mathbf{R} - c_S c_u \mathbf{I}_m$ , and  $c_S := \frac{\min(\lambda_{\min}(\mathbf{Q}), \lambda_{\min}(\mathbf{R}))}{\max(c_u, c_y)}$ , for all  $[\tilde{\mathbf{A}} \ \tilde{\mathbf{B}}] \in \tilde{\mathbf{A}}$  from Assumption 5.

*Proof:* Let us first consider the case where the candidate solution (49) for time-step  $k+1$  is feasible. We can then bound the expected cost increase as

$$\begin{aligned} & \mathbb{E} [J_{T_f}^*(\boldsymbol{\xi}_{k+1}) \mid \tilde{\mathbf{v}}_{f,k+1} \text{ feasible}] - J_{T_f}^*(\boldsymbol{\xi}_k) \\ & \leq \mathbb{E} [J_{T_f}(\boldsymbol{\xi}_{k+1}, \tilde{\mathbf{v}}_{f,k+1})] - J_{T_f}^*(\boldsymbol{\xi}_k) \end{aligned} \quad (52)$$

$$\begin{aligned} & = \mathbb{E} \left[ \sum_{l=1}^{T_f} \left( \left\| \mathbf{y}_{l|k}^* + \tilde{\mathbf{E}}^\top \tilde{\mathbf{A}}_{\text{cl}}^l \tilde{\mathbf{E}} \mathbf{d}_k \right\|_Q^2 \right. \right. \\ & \quad \left. \left. + \left\| \mathbf{u}_{l|k}^* + \mathbf{K} \tilde{\mathbf{A}}_{\text{cl}}^{l-1} \tilde{\mathbf{E}} \mathbf{d}_k \right\|_R^2 \right) + \left\| \tilde{\mathbf{A}}_{\text{cl}} \boldsymbol{\xi}_{T_f|k}^* + \tilde{\mathbf{A}}_{\text{cl}}^{T_f} \tilde{\mathbf{E}} \mathbf{d}_k \right\|_P^2 \right] \\ & \quad - \mathbb{E} \left[ \sum_{l=0}^{T_f-1} \left( \left\| \mathbf{y}_{l|k}^* \right\|_Q^2 + \left\| \mathbf{u}_{l|k}^* \right\|_R^2 \right) + \left\| \boldsymbol{\xi}_{T_f|k}^* \right\|_P^2 \right] \end{aligned} \quad (53)$$

$$\begin{aligned} & \leq \mathbb{E} \left[ \sum_{l=1}^{T_f} \left( \left\| \tilde{\mathbf{E}}^\top \tilde{\mathbf{A}}_{\text{cl}}^l \tilde{\mathbf{E}} \mathbf{d}_k \right\|_Q^2 + \left\| \mathbf{K} \tilde{\mathbf{A}}_{\text{cl}}^{l-1} \tilde{\mathbf{E}} \mathbf{d}_k \right\|_R^2 \right) \right. \\ & \quad \left. + \left\| \tilde{\mathbf{A}}_{\text{cl}}^{T_f} \tilde{\mathbf{E}} \mathbf{d}_k \right\|_P^2 \right] - \mathbb{E} \left[ \left\| \mathbf{y}_{0|k}^* \right\|_Q^2 + \left\| \mathbf{u}_{0|k}^* \right\|_R^2 + \left\| \boldsymbol{\xi}_{T_f|k}^* \right\|_P^2 \right] \\ & \quad + \mathbb{E} \left[ \left\| \mathbf{y}_{T_f|k}^* \right\|_Q^2 + \left\| \mathbf{u}_{T_f|k}^* \right\|_R^2 + \left\| \tilde{\mathbf{A}}_{\text{cl}} \boldsymbol{\xi}_{T_f|k}^* \right\|_P^2 \right] \end{aligned} \quad (54)$$

$$\begin{aligned} & \leq \mathbb{E} \left[ \left\| \tilde{\mathbf{E}} \mathbf{d}_k \right\|_P^2 \right] - \mathbb{E} \left[ \left\| \mathbf{y}_{0|k}^* \right\|_Q^2 + \left\| \mathbf{u}_{0|k}^* \right\|_R^2 + \left\| \boldsymbol{\xi}_{T_f|k}^* \right\|_P^2 \right] \\ & \quad + \mathbb{E} \left[ \left\| \tilde{\mathbf{E}}^\top \tilde{\mathbf{A}}_{\text{cl}} \boldsymbol{\xi}_{T_f|k}^* \right\|_Q^2 + \left\| \mathbf{K} \boldsymbol{\xi}_{T_f|k}^* \right\|_R^2 + \left\| \tilde{\mathbf{A}}_{\text{cl}} \boldsymbol{\xi}_{T_f|k}^* \right\|_P^2 \right] \end{aligned} \quad (55)$$

$$\leq \mathbb{E} \left[ \left\| \tilde{\mathbf{E}} \mathbf{d}_k \right\|_P^2 - \left\| \mathbf{y}_{0|k}^* \right\|_Q^2 - \left\| \mathbf{u}_{0|k}^* \right\|_R^2 \right], \quad (56)$$

using the Cauchy-Schwarz inequality and Assumption 5(b). For the case where the candidate solution (49) for time-step  $k+1$  is infeasible, we bound the expected cost increase as

$$\begin{aligned} & \mathbb{E} [J_{T_f}^*(\boldsymbol{\xi}_{k+1}) \mid \tilde{\mathbf{v}}_{f,k+1} \text{ infeasible}] - J_{T_f}^*(\boldsymbol{\xi}_k) \\ & \leq \mathbb{E} \left[ \max_{[\tilde{\mathbf{A}} \ \tilde{\mathbf{B}}] \in \tilde{\mathbf{A}}} \left\| \tilde{\mathbf{A}} \boldsymbol{\xi}_k + \tilde{\mathbf{B}} \mathbf{u}_k + \tilde{\mathbf{E}} \mathbf{d}_k \right\|_{\mathbf{P}_u}^2 - \|\boldsymbol{\xi}_k\|_{\mathbf{P}_1}^2 \right] \end{aligned} \quad (57)$$

$$\leq \mathbb{E} \left[ \max_{[\tilde{\mathbf{A}} \ \tilde{\mathbf{B}}] \in \tilde{\mathbf{A}}} \left\| [\tilde{\mathbf{A}} \ \tilde{\mathbf{B}}] \begin{bmatrix} \boldsymbol{\xi}_k \\ \mathbf{u}_k \end{bmatrix} \right\|_{\mathbf{P}_u}^2 - \|\boldsymbol{\xi}_k\|_{\mathbf{P}_1}^2 + \left\| \tilde{\mathbf{E}} \mathbf{d}_k \right\|_{\mathbf{P}_u}^2 \right], \quad (58)$$

using Assumption 6. Thus, applying the law of total probability, we retrieve

$$\begin{aligned} & \mathbb{E} [J_{T_f}^*(\boldsymbol{\xi}_{k+1})] - J_{T_f}^*(\boldsymbol{\xi}_k) \\ & \leq (1 - \varepsilon_f) \mathbb{E} \left[ \left\| \tilde{\mathbf{E}} \mathbf{d}_k \right\|_P^2 - \left\| \mathbf{y}_{0|k}^* \right\|_Q^2 - \left\| \mathbf{u}_{0|k}^* \right\|_R^2 \right] \\ & \quad + \varepsilon_f \mathbb{E} \left[ \max_{[\tilde{\mathbf{A}} \ \tilde{\mathbf{B}}] \in \tilde{\mathbf{A}}} \left\| [\tilde{\mathbf{A}} \ \tilde{\mathbf{B}}] \begin{bmatrix} \boldsymbol{\xi}_k \\ \mathbf{u}_k \end{bmatrix} \right\|_{\mathbf{P}_u}^2 - \|\boldsymbol{\xi}_k\|_{\mathbf{P}_1}^2 + \left\| \tilde{\mathbf{E}} \mathbf{d}_k \right\|_{\mathbf{P}_u}^2 \right]. \end{aligned} \quad (59)$$

Now, as a stochastic ISS Lyapunov function candidate, we define  $V(\boldsymbol{\xi}_k) := J_{T_f}^*(\boldsymbol{\xi}_k) - c + (1 - \varepsilon_f) c_S W(\boldsymbol{\xi}_k)$ . By combining (50) and (59), we retrieve for the expected descent

of the Lyapunov function candidate

$$\begin{aligned} & E[V(\boldsymbol{\xi}_{k+1})] - V(\boldsymbol{\xi}_k) \\ & \leq (1 - \varepsilon_f) E \left[ \left\| \tilde{\mathbf{E}} \mathbf{d}_k \right\|_P^2 - \left\| \mathbf{y}_{0|k}^* \right\|_Q^2 - \left\| \mathbf{u}_k \right\|_R^2 \right] \\ & \quad + \varepsilon_f E \left[ \max_{[\tilde{\mathbf{A}} \ \tilde{\mathbf{B}}] \in \tilde{\mathcal{A}}} \left\| [\tilde{\mathbf{A}} \ \tilde{\mathbf{B}}] \begin{bmatrix} \boldsymbol{\xi}_k \\ \mathbf{u}_k \end{bmatrix} \right\|_{P_u}^2 - \left\| \boldsymbol{\xi}_k \right\|_{P_1}^2 + \left\| \tilde{\mathbf{E}} \mathbf{d}_k \right\|_{P_u}^2 \right] \\ & \quad + (1 - \varepsilon_f) E \left[ c_{S c_u} \left\| \mathbf{u}_k \right\|^2 + c_{S c_y} \left\| \mathbf{y}_k \right\|^2 + c_{S c_d} \left\| \mathbf{d}_k \right\|^2 \right] \\ & \quad - (1 - \varepsilon_f) \frac{c_S}{2} \left\| \boldsymbol{\xi}_k \right\|^2 \end{aligned} \quad (60)$$

$$\begin{aligned} & \leq E \left[ \left\| \mathbf{d}_k \right\|_{P_d}^2 \right] - (1 - \varepsilon_f) \left( \frac{c_S}{2} \left\| \boldsymbol{\xi}_k \right\|^2 + \left\| \mathbf{u}_k \right\|_{R - c_{S c_u} I_m}^2 \right. \\ & \quad \left. - \frac{\varepsilon_f}{1 - \varepsilon_f} \max_{[\tilde{\mathbf{A}} \ \tilde{\mathbf{B}}] \in \tilde{\mathcal{A}}} \left\| [\tilde{\mathbf{A}} \ \tilde{\mathbf{B}}] \begin{bmatrix} \boldsymbol{\xi}_k \\ \mathbf{u}_k \end{bmatrix} \right\|_{P_u}^2 - \left\| \boldsymbol{\xi}_k \right\|_{P_1}^2 \right) \end{aligned} \quad (61)$$

$$\leq - (1 - \varepsilon_f) \lambda_{\min}(\mathbf{Q}_S) \left\| \boldsymbol{\xi}_k \right\|^2 + \lambda_{\max}(\mathbf{P}_d) \text{tr}(\boldsymbol{\Sigma}), \quad (62)$$

with  $\mathbf{P}_d := \tilde{\mathbf{E}}^\top ((1 - \varepsilon_f) \mathbf{P} + \varepsilon_f \mathbf{P}_u) \tilde{\mathbf{E}} + c_{S c_d} I_p$  and  $\mathbf{Q}_S$  from (51). If  $\mathbf{Q}_S \succ \mathbf{0}$  for all  $[\tilde{\mathbf{A}} \ \tilde{\mathbf{B}}] \in \tilde{\mathcal{A}}$ , property (48b) is satisfied for  $\varrho_3(\|\boldsymbol{\xi}_k\|) = (1 - \varepsilon_f) \lambda_{\min}(\mathbf{Q}_S) \|\boldsymbol{\xi}_k\|^2$  and  $\varrho_5(\text{tr}(\boldsymbol{\Sigma})) = \lambda_{\max}(\mathbf{P}_d) \text{tr}(\boldsymbol{\Sigma})$ . Furthermore, property (48a) holds for  $\varrho_1(\|\boldsymbol{\xi}_k\|) = \|\boldsymbol{\xi}_k\|_{P_1}^2$ ,  $\varrho_2(\|\boldsymbol{\xi}_k\|) = \|\boldsymbol{\xi}_k\|_{P_u + P_w}^2$ , and arbitrary  $\varrho_4 \in \mathcal{H}$ . Therefore,  $V(\boldsymbol{\xi}_k)$  is a valid stochastic ISS Lyapunov function on  $\mathcal{C}_\xi^\infty$ , which concludes the proof. ■

**Remark 7** For the trivial case  $\varepsilon_f = 0$  (i.e., the candidate solution (49) is always feasible),  $\mathbf{Q}_S \succ \mathbf{0}$  holds by design.

We close this section by remarking that a similar bound as in (47) can be given for the output  $\mathbf{y}_k$  using  $\mathbf{y}_k = \tilde{\mathbf{E}}^\top \boldsymbol{\xi}_{k+1}$ .

## VI. NUMERICAL EVALUATION

In this section, we evaluate the proposed data-driven sample-based predictors and the proposed control algorithm on an example system in simulation.

### A. Simulation Setup

The considered example system, i.e., a linearized DC-DC converter [40], is modelled by (2) with  $T_p = 1$  and

$$\Phi = \begin{bmatrix} 4.697 & 1 & 0.073 \\ 0.083 & -0.060 & 0.997 \end{bmatrix}, \quad \Psi = \mathbf{0}. \quad (63)$$

The system is subject to polytopic input and output constraints of the form (8) with  $\mathbf{G}_u = \text{col}(\mathbf{I}_m, -\mathbf{I}_m)$ ,  $\mathbf{g}_u = 0.2 \cdot \mathbf{1}_{2m}$ ,  $\mathbf{G}_y = \text{col}(\mathbf{I}_p, -\mathbf{I}_p)$ ,  $\mathbf{g}_y = 3 \cdot \mathbf{1}_{2p}$ . The polytopic disturbance bound is given as in (7) with  $\mathbf{G}_d = \text{col}(\mathbf{I}_p, -\mathbf{I}_p)$ ,  $\mathbf{g}_d = \mathbf{1}_2 \otimes [0.1 \ 0.05]^\top$ . The disturbance is distributed uniformly within the bounds.

For the data collection (see Assumption 3), we apply random admissible inputs and record an input-output trajectory of length  $T = 55$ . For the cost function (9), we choose a prediction horizon of  $T_f = 6$  and the input and output weighting matrices

$$\mathbf{R} = 1, \quad \mathbf{Q} = \begin{bmatrix} 1 & 0 \\ 0 & 100 \end{bmatrix}. \quad (64)$$

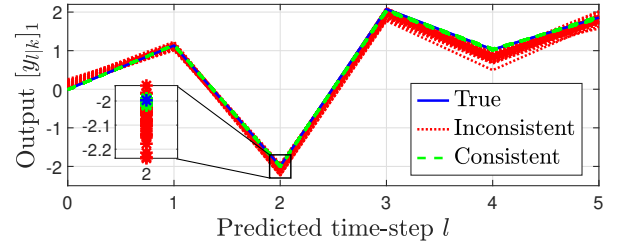


Fig. 2. Comparison of sampled output predictions and true output trajectory (blue) for predictors based on consistently (green) and inconsistently (red) sampled disturbance data.

The pre-stabilizing state-feedback gain  $\mathbf{K}$ , terminal weighting matrix  $\mathbf{P}$ , and terminal set  $\mathbb{X}_{T_f}$  are computed as in Appendix I, yielding  $\mathbf{K} = [-1.21 \ -0.27 \ 0.04]$  and

$$\mathbf{P} = \begin{bmatrix} 152.31 & 72.98 & -525.09 \\ 72.98 & 28.13 & -292.72 \\ -525.09 & -292.72 & 2345.46 \end{bmatrix}. \quad (65)$$

### B. Open-loop Results

We first evaluate the open-loop prediction accuracy of the data-driven sample-based output predictor (29) when using consistent disturbance data samples compared to inconsistently sampled data (i.e., not considering the consistency constraint (15)). To do so, we set  $\boldsymbol{\xi}_k = \mathbf{0}$  and generate 100 random admissible input sequences  $\mathbf{v}_{f,k}$ . For every input sequence, we draw 1000 random disturbance data samples  $\mathcal{D}^{(i)}$ , and compute the corresponding output prediction  $\mathbf{y}_{f,k}^{(i)}$  using (29) with  $\mathbf{d}_{f,k}^{(i)} = \mathbf{0}$ . Then, for both consistently and inconsistently sampled disturbance data  $\mathcal{D}^{(i)}$ , we compute the root-mean-square error (RMSE) between the sampled output predictions and the true output trajectory that would result from applying the given input sequence. An example scenario is depicted in Fig. 2. For this simulation example, predictors based on consistently sampled disturbance data emit a mean reduction in RMSE of 77.37% compared to using inconsistent samples, with minimal and maximal reduction of 52.13% and 90.18%, respectively.

### C. Closed-loop Results

We now evaluate the performance of the proposed controller for both constraint sampling approaches presented in Appendix III. The control goal is to stabilize the system around the origin, starting from  $\boldsymbol{\xi}_0 := \text{col}(0, 0, 2.8)$ , while satisfying constraints (8). In a Monte-Carlo simulation of 100 runs, the proposed controller is applied for 30 time-steps, where at each time-step a new randomly generated disturbance realization affects the system. The simulations are carried out in MATLAB using the `quadprog` solver.

For the constraint sampling, we choose the risk parameter  $\varepsilon = 0.05$  and confidence  $\varepsilon^c = 10^{-4}$ . By Proposition 4, the direct approximation approach requires 17 350 to 42 363 samples per prediction stage for the  $\varepsilon$ -CSS approximation, leading to a constraint set (35) consisting of 1 443 456 linear inequalities. In contrast, by Proposition 5, the probabilistic

scaling approach requires 1 375 samples per prediction stage. To retrieve suitable candidate SASSs, we use 5 000 to 10 000 “design” samples (see Sec. IV-B), leading to 360 000 inequalities. After removing redundant constraints, we end up with 1 212 inequalities for the direct approximation approach and 789 inequalities for the probabilistic scaling approach.

Fig. 3 shows trajectories from 20 exemplary runs of the controller based on the direct approximation approach. The probabilistic constraint tightening of the proposed scheme allows the system to operate close to the constraint boundary, leading to fast convergence. No constraint violations occur in any run for the two sampling approaches due to the conservatism of both the robust first-step constraint and the sampling-based  $\varepsilon$ -CSS approximation. The mean computation time for solving the OCP (41) per time-step on an AMD Ryzen 5 Pro 3500U results in 0.98 ms for the controller based on direct approximation, and 0.88 ms for the controller based on probabilistic scaling.

Next, we evaluate the total trajectory costs

$$J_{\text{tot}} = \sum_{k=0}^{29} (\mathbf{y}_k^\top \mathbf{Q} \mathbf{y}_k + \mathbf{u}_k^\top \mathbf{R} \mathbf{u}_k) \quad (66)$$

of the proposed controller. When using the direct approximation approach for the controller, we retrieve minimal, mean, and maximal trajectory costs of 3 746, 4 453, and 5 140, respectively. While the probabilistic scaling approach requires fewer samples, the corresponding controller based on probabilistic scaling results in slightly higher trajectory costs for this example, namely minimal, mean, and maximal costs increase of 0.72 %, 0.86 %, and 1.05 %, respectively.

Finally, we comment on validity of Theorem 2, which depends on the probability  $\varepsilon_f$  of infeasibility of the candidate solution (49) provided in Definition 4. Since  $\varepsilon_f$  cannot be determined a priori, we evaluate  $\varepsilon_f$  practically by checking feasibility of the candidate solution (49) in every control iteration of each Monte Carlo run. For both considered sampling-based controllers, the candidate solution is feasible in every iteration. Thus,  $\varepsilon_f = 0$ , and the origin is RASiE by Theorem 2.

## VII. CONCLUSION

In this paper, we proposed a stochastic output-feedback DPC scheme for the model-free control of LTI systems subject to bounded additive disturbances and probabilistic chance constraints. A single persistently exciting input-output data trajectory is used as a basis for the provided data-driven multi-step predictors. The proposed approach only requires bounds and distributional knowledge of the disturbance, opposed to related approaches that additionally rely on exact disturbance measurements. By employing a sampling-based approach and by leveraging a novel parameterization of the set of unknown consistent disturbance data, we derived a deterministic approximation of the chance constraints. The parameterization of the consistent disturbance data naturally allows for incorporation of prior model knowledge to further reduce conservatism. Recursive feasibility and closed-loop constraint satisfaction are guaranteed by employing a robust first-step constraint. We proved robust asymptotic stability in expectation of the closed-loop system depending on the probability of infeasibility of a

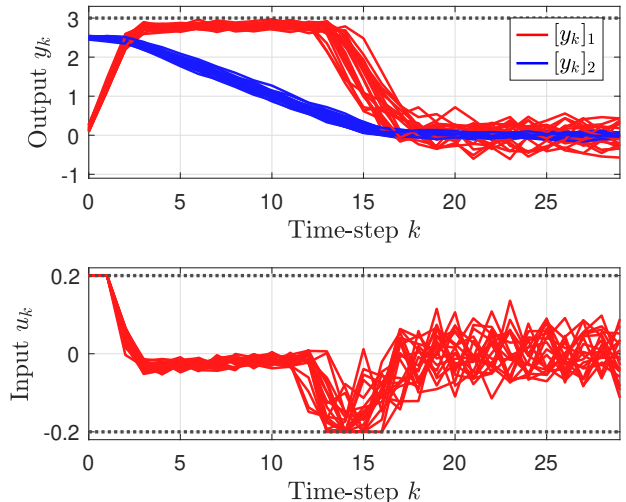


Fig. 3. Trajectories of 20 exemplary runs subject to random disturbances. Constraints are shown in dotted black lines.

candidate solution as common in sampling-based stochastic MPC literature [15], [17] and under standard assumptions on stabilizing ingredients that are determinable from the available data. Performing all computationally challenging tasks offline before the control phase leads to a lightweight online DPC scheme. A numerical example demonstrates the efficiency of the proposed controller for different sampling approaches, as well as improvement in prediction accuracy when using the proposed data-driven predictors based on consistent disturbance data samples.

In future work, we will explore adaptation of the set of consistent disturbance data online using newly retrieved input-output data, potentially leading to reduced data uncertainty and thus improved control, similar to adaptive MPC [33], [34]. In order to improve scalability of the control scheme, it is of interest to investigate the use of configuration-constrained polytopes [41] as candidate simple approximating sets, reducing the complexity of the first-step constraint computation.

## APPENDIX I

### DATA-DRIVEN DESIGN OF TERMINAL INGREDIENTS

Here, we describe approaches on how to determine a stabilizing feedback gain  $\mathbf{K}$ , weighting matrix  $\mathbf{P}$ , and terminal set  $\mathbb{X}_{T_f}$  from Assumption 5, given data from Assumption 3.

a) *Stabilizing feedback gain  $\mathbf{K}$* : The feedback gain  $\mathbf{K}$  should be chosen such that  $\mathbf{A}_{\text{cl},j} := \tilde{\mathbf{A}}_j + \mathbf{K} \tilde{\mathbf{B}}_j$  is Schur stable for all  $j \in \mathbb{N}_1^{N_v}$ , see Assumption 5(a). From [8, Lemma 3],  $\tilde{\mathbf{A}}_{\text{cl},j}$  can be equivalently described as

$$\tilde{\mathbf{A}}_{\text{cl},j} = \mathbf{H}_{\xi,j}^+ \Theta, \quad (67)$$

with  $\mathbf{H}_{\xi,j}^+ := [\xi_2^d \cdots \xi_{T+1}^d] - \tilde{\mathbf{E}} \mathbf{H}_1(\mathcal{D}_{T,j})$  and for some  $\Theta$  that satisfies

$$\begin{bmatrix} \mathbf{H}_1(\mathcal{X}_T) \\ \mathbf{H}_1(\mathcal{U}_T) \end{bmatrix} \Theta = \begin{bmatrix} \mathbf{I}_{n_\varepsilon} \\ \mathbf{K} \end{bmatrix}, \quad (68)$$

where  $\mathcal{D}_{T,j}$  is constructed using (17) and the vertex  $\mathcal{D}_{n_\varepsilon+m,j}$  from the set of consistent disturbance data (22). Following

ideas from [25], a feedback gain  $\mathbf{K}$  that stabilizes all  $\tilde{\mathbf{A}}_{\text{cl},j}$ ,  $j \in \mathbb{N}_1^{N_v}$ , can be found by solving the linear matrix inequalities

$$\begin{bmatrix} \mathbf{H}_1(\mathcal{X}_T) \Theta & \mathbf{H}_{\xi,j}^+ \Theta \\ \left( \mathbf{H}_{\xi,j}^+ \Theta \right)^\top & \mathbf{H}_1(\mathcal{X}_T) \Theta \end{bmatrix} \succ \mathbf{0} \quad \forall j \in \mathbb{N}_1^{N_v} \quad (69)$$

for  $\Theta$ , resulting in  $\mathbf{K} = \mathbf{H}_1(\mathcal{U}_T) \Theta (\mathbf{H}_1(\mathcal{X}_T) \Theta)^{-1}$ .

b) *Weighting matrix P*: The matrix  $\mathbf{P}$  should be chosen such that Assumption 5(b) holds for given weights  $\mathbf{Q}$ ,  $\mathbf{R}$  and feedback gain  $\mathbf{K}$ . With the matrix vertices  $\tilde{\mathbf{A}}_{\text{cl},j}$ ,  $j \in \mathbb{N}_1^{N_v}$ , we can find a matrix  $\mathbf{P}$  that satisfies Assumption 5(b) by solving

$$\underset{\tilde{\mathbf{P}}}{\text{minimize}} \quad \text{trace}(\tilde{\mathbf{P}}) \quad (70a)$$

$$\text{s.t.} \quad \begin{bmatrix} \tilde{\mathbf{P}} - \mathbf{Q}_P & \tilde{\mathbf{A}}_{\text{cl},j}^\top \tilde{\mathbf{P}} \\ \tilde{\mathbf{P}} \tilde{\mathbf{A}}_{\text{cl},j} & \tilde{\mathbf{P}} \end{bmatrix} \succ \mathbf{0} \quad \forall j \in \mathbb{N}_1^{N_v}, \quad (70b)$$

$$\tilde{\mathbf{P}} - \mathbf{Q}_P \succ \mathbf{0}, \quad (70c)$$

with  $\mathbf{Q}_P := \mathbf{K}^\top \mathbf{R} \mathbf{K} + \tilde{\mathbf{E}} \mathbf{Q} \tilde{\mathbf{E}}^\top$ ,  $\mathbf{P} = \tilde{\mathbf{P}} - \tilde{\mathbf{E}} \mathbf{Q} \tilde{\mathbf{E}}^\top$ . We remark that (69) and (70) can be simplified by over-approximating the set of matrix vertices (23) via interval matrices, and then using the result from [42] to reduce the number of to-be-checked vertices.

c) *Terminal set  $\mathbb{X}_{T_f}$* : First, let us denote the constraint set of the extended state  $\xi$  as  $\mathbb{X} := \{\xi \in \mathbb{R}^{n_\xi} \mid \mathbf{G}_\xi \xi \leq \mathbf{g}_\xi\}$ . The set  $\mathbb{X}$  can be constructed by considering the in- and output constraints (8) as well as the definition of the extended state in (3). The terminal set  $\mathbb{X}_{T_f}$  is defined as a subset of  $\mathbb{X}$  that is RPI under the control law  $\mathbf{u}_k = \mathbf{K} \xi_k$ . According to [35], we can make use of the given matrix vertices  $\tilde{\mathbf{A}}_{\text{cl},j}$ ,  $j \in \mathbb{N}_1^{N_v}$  and disturbance bound  $\mathbb{D}$  from (7) to determine  $\mathbb{X}_{T_f}$  through  $\mathbb{X}_{T_f} = \bigcap_{i=0}^{\infty} \mathbb{X}^i$ , with  $\mathbb{X}^0 = \mathbb{X}$  and

$$\mathbb{X}^{i+1} = \left\{ \xi \in \mathbb{X}^i \mid \forall d \in \mathbb{D}, j \in \mathbb{N}_1^{N_v} : \mathbf{K} \xi \in \mathbb{U}, \tilde{\mathbf{A}}_{\text{cl},j} \xi + \tilde{\mathbf{E}} d \in \mathbb{X}^i \right\}. \quad (71)$$

In practice, the recursion (71) is terminated once  $\mathbb{X}^{i+1} = \mathbb{X}^i$  for some  $i \in \mathbb{N}$ , yielding  $\mathbb{X}_{T_f} = \mathbb{X}^i$ . Note that, as  $\mathbb{D}$  is polytopic, it is sufficient to only take its vertices into account.

## APPENDIX II PARAMETERS OF DATA-DRIVEN PREDICTORS

Here, we describe how the parameters  $\mathbf{M}_y^{(i)}$ ,  $\mathbf{m}_y^{(i)}$ ,  $\mathbf{M}_u^{(i)}$ ,  $\mathbf{m}_u^{(i)}$ ,  $\mathbf{M}_\xi^{(i)}$ ,  $\mathbf{m}_\xi^{(i)}$  from (29) and (30) depend on the uncertainty samples  $\mathbf{d}_{f,k}^{(i)}$ ,  $\mathcal{D}_T^{(i)}$  and the data from Assumption 3.

With  $\tilde{T} := T - T_f + 1$ , let us define the data matrices

$$\mathbf{\Pi}_{\xi,v} := \mathbf{I}_{\tilde{T}} - \begin{bmatrix} \mathbf{H}_1(\mathcal{X}_{\tilde{T}}) \\ \mathbf{H}_{T_f}(\mathcal{V}_T) \end{bmatrix}^\dagger \begin{bmatrix} \mathbf{H}_1(\mathcal{X}_{\tilde{T}}) \\ \mathbf{H}_{T_f}(\mathcal{V}_T) \end{bmatrix}, \quad (72a)$$

$$\mathbf{\Pi}_d^{(i)} := \mathbf{I}_{\tilde{T}} - \mathbf{H}_{T_f}(\mathcal{D}_T^{(i)})^\dagger \mathbf{H}_{T_f}(\mathcal{D}_T^{(i)}). \quad (72b)$$

With (72), we can reformulate (28) into

$$\begin{aligned} \boldsymbol{\alpha}^{(i)} &= \left( \begin{bmatrix} \mathbf{H}_1(\mathcal{X}_{\tilde{T}}) \\ \mathbf{H}_{T_f}(\mathcal{V}_T) \end{bmatrix} \mathbf{\Pi}_d^{(i)} \right)^\dagger \begin{bmatrix} \boldsymbol{\xi}_k \\ \mathbf{v}_{f,k} \end{bmatrix} \\ &+ \left( \mathbf{H}_{T_f}(\mathcal{D}_T^{(i)}) \mathbf{\Pi}_{\xi,v} \right)^\dagger \mathbf{d}_{f,k}^{(i)}. \end{aligned} \quad (73)$$

Inserting (73) into (13b) yields the output predictor (29) with

$$\mathbf{M}_y^{(i)} := \mathbf{H}_{T_f}(\mathcal{Y}_T) \left( \begin{bmatrix} \mathbf{H}_1(\mathcal{X}_{\tilde{T}}) \\ \mathbf{H}_{T_f}(\mathcal{V}_T) \end{bmatrix} \mathbf{\Pi}_d^{(i)} \right)^\dagger, \quad (74a)$$

$$\mathbf{m}_y^{(i)} := \mathbf{H}_{T_f}(\mathcal{Y}_T) \left( \mathbf{H}_{T_f}(\mathcal{D}_T^{(i)}) \mathbf{\Pi}_{\xi,v} \right)^\dagger \mathbf{d}_{f,k}^{(i)}. \quad (74b)$$

Similarly, by using (73) and (13b), and by considering the decomposition (12), we retrieve the input predictor (30) with

$$\mathbf{M}_u^{(i)} := \mathbf{H}_{T_f}(\mathcal{U}_T) \left( \begin{bmatrix} \mathbf{H}_1(\mathcal{X}_{\tilde{T}}) \\ \mathbf{H}_{T_f}(\mathcal{V}_T) \end{bmatrix} \mathbf{\Pi}_d^{(i)} \right)^\dagger, \quad (75a)$$

$$\mathbf{m}_u^{(i)} := \mathbf{H}_{T_f}(\mathcal{U}_T) \left( \mathbf{H}_{T_f}(\mathcal{D}_T^{(i)}) \mathbf{\Pi}_{\xi,v} \right)^\dagger \mathbf{d}_{f,k}^{(i)}. \quad (75b)$$

Analogously, we retrieve the data-driven sample-based predictor (31) of the terminal extended state with the parameters

$$\mathbf{M}_\xi^{(i)} := [\boldsymbol{\xi}_{T_f}^d \cdots \boldsymbol{\xi}_T^d] \left( \begin{bmatrix} \mathbf{H}_1(\mathcal{X}_{\tilde{T}}) \\ \mathbf{H}_{T_f}(\mathcal{V}_T) \end{bmatrix} \mathbf{\Pi}_d^{(i)} \right)^\dagger, \quad (76a)$$

$$\mathbf{m}_\xi^{(i)} := [\boldsymbol{\xi}_{T_f}^d \cdots \boldsymbol{\xi}_T^d] \left( \mathbf{H}_{T_f}(\mathcal{D}_T^{(i)}) \mathbf{\Pi}_{\xi,v} \right)^\dagger \mathbf{d}_{f,k}^{(i)}. \quad (76b)$$

## APPENDIX III SAMPLING-BASED APPROXIMATION OF $\varepsilon$ -CCS

Here, we briefly present two popular approaches and the relevant theory for sampling-based inner-approximations of an  $\varepsilon$ -CCS. For a more general discussion, see [16].

Consider a general joint chance constraint  $\Pr[\mathbf{G}_\zeta(\mathbf{w})\boldsymbol{\zeta} \leq \mathbf{g}_\zeta(\mathbf{w})] \geq 1 - \varepsilon$  where  $\boldsymbol{\zeta}$  is the (deterministic) decision variable, and  $\mathbf{G}_\zeta(\mathbf{w}) \in \mathbb{R}^{n_c \times n_c}$ ,  $\mathbf{g}_\zeta(\mathbf{w}) \in \mathbb{R}^{n_c}$  are constraint parameters that depend on the realization  $\mathbf{w} \in \mathbb{R}^{n_w}$  of a multivariate random variable. The corresponding  $\varepsilon$ -CCS is defined as

$$\mathbb{Z}^P = \{\boldsymbol{\zeta} \in \mathbb{R}^{n_c} \mid \Pr[\mathbf{G}_\zeta(\mathbf{w})\boldsymbol{\zeta} \leq \mathbf{g}_\zeta(\mathbf{w})] \geq 1 - \varepsilon\}. \quad (77)$$

The goal of offline-sampling-based approaches is to determine a deterministic inner-approximation  $\mathbb{Z}^S$  of the  $\varepsilon$ -CCS (77) by using  $N_s$  iid uncertainty samples  $\mathbf{w}^{(i)}$ ,  $i \in \mathbb{N}_1^{N_s}$ , yielding  $\Pr[\mathbb{Z}^S \subseteq \mathbb{Z}^P] \geq 1 - \varepsilon^c$  with user-chosen confidence  $\varepsilon^c$ . The two popular approaches presented in the following, namely the direct sampling-based approximation and the probabilistic scaling approach, make use of the sampled set corresponding to (77), i.e. (for a given sample  $\mathbf{w}^{(i)}$ )

$$\tilde{\mathbb{Z}}^S(\mathbf{w}^{(i)}) = \left\{ \boldsymbol{\zeta} \in \mathbb{R}^{n_c} \mid \mathbf{G}_\zeta(\mathbf{w}^{(i)})\boldsymbol{\zeta} \leq \mathbf{g}_\zeta(\mathbf{w}^{(i)}) \right\}. \quad (78)$$

### A. Direct Sampling-based Approximation

For the direct sampling-based approximation of the  $\varepsilon$ -CCS (77), the  $N_s$  samples of  $\mathbf{w}$  and (78) are used to define the sampled set  $\mathbb{Z}_{\text{LT}}^S := \bigcap_{i=0}^{N_s} \tilde{\mathbb{Z}}^S(\mathbf{w}^{(i)})$ . The following result from statistical learning theory [43] allows us to determine the required number of samples  $N_s$  (i.e., the sample complexity) for which the sampled set  $\mathbb{Z}_{\text{LT}}^S$  is a subset of the  $\varepsilon$ -CCS (77) with a predefined confidence  $\varepsilon^c$ .

**Proposition 4 (Learning Theory Bound [16])** *For any risk parameter  $\varepsilon \in (0, 0.14)$ , confidence level  $\varepsilon^c \in (0, 1)$ , and sample complexity  $N_s \geq N_{\text{LT}}(\varepsilon, \varepsilon^c, n_\zeta, n_c)$  with*

$$N_{\text{LT}} := \frac{4.1}{\varepsilon} \left( \ln \frac{21.64}{\varepsilon^c} + 4.39 n_\zeta \log_2 \frac{8 \varepsilon n_c}{\varepsilon} \right) \quad (79)$$

and Euler's number  $e$ , it holds that  $\Pr [\mathbb{Z}_{\text{LT}}^{\text{S}} \subseteq \mathbb{Z}^{\text{P}}] \geq 1 - \varepsilon^c$ .

Application of Proposition 4 in the context of sampling-based Stochastic MPC was first presented in [15] for the case of single chance constraints (i.e.,  $n_c = 1$ ). A disadvantage of Proposition 4 is that the sample complexity bound (79) is rather conservative, easily leading to millions of sampled constraints even for small-scale systems [16]. Although the sampled constraints in (78) are generally highly redundant and can be reduced offline [15], the final number of constraints might still be too large to guarantee real-time implementability of the resulting predictive controller. For this reason, approaches have emerged that probabilistically scale a pre-defined set of fixed complexity to retrieve an inner-approximations of the  $\varepsilon$ -CSS (77), as presented next.

### B. Approximation via Probabilistic Scaling

This approach is based on the idea of approximating the  $\varepsilon$ -CSS (77) via a scalable SAS

$$\mathbb{Z}^{\text{S}}(\sigma) := \{\zeta_c\} \oplus \sigma \mathbb{Z}^{\text{SAS}}, \quad (80)$$

with the center  $\zeta_c$ , the shape  $\mathbb{Z}^{\text{SAS}}$ , and the scaling factor  $\sigma \geq 0$ . The designer controls the complexity of the approximating set by suitable choice of the design parameters  $\zeta_c, \mathbb{Z}^{\text{SAS}}$ .

The goal of the probabilistic scaling approach is to find an optimal scaling factor  $\sigma^*$  such that  $\Pr [\mathbb{Z}^{\text{S}}(\sigma^*) \subseteq \mathbb{Z}^{\text{P}}] \geq 1 - \varepsilon^c$  with a desired level of confidence  $\varepsilon^c$  by exploiting samples. Before we can state the probabilistic scaling approach, consider the following definition of the scaling factor.

**Definition 5 (Scaling Factor [16])** For a given SAS  $\mathbb{Z}^{\text{S}}(\sigma)$  with center  $\zeta_c$  and shape  $\mathbb{Z}^{\text{SAS}}$ , and a sample  $\mathbf{w}$ , the scaling factor  $\sigma(\mathbf{w})$  of  $\mathbb{Z}^{\text{S}}(\sigma)$  relative to  $\mathbf{w}$  is defined as

$$\sigma(\mathbf{w}) := \begin{cases} \max_{\mathbb{Z}^{\text{S}}(\sigma) \subseteq \tilde{\mathbb{Z}}^{\text{S}}(\mathbf{w})} \sigma & \text{if } \zeta_c \in \tilde{\mathbb{Z}}^{\text{S}}(\mathbf{w}) \\ 0 & \text{otherwise.} \end{cases} \quad (81)$$

**Proposition 5 (Probabilistic Scaling of SAS [16])** For a given candidate SAS  $\mathbb{Z}^{\text{S}}(\sigma)$  with center  $\zeta_c \in \mathbb{Z}^{\text{P}}$ , any risk parameter  $\varepsilon \in (0, 1)$ , and confidence level  $\varepsilon^c \in (0, 1)$ , let the sample complexity  $N_s$  be chosen as  $N_s \geq N_{\text{PS}}(\varepsilon, \varepsilon^c)$ , with

$$N_{\text{PS}} := \frac{7.47}{\varepsilon} \ln \frac{1}{\varepsilon^c}. \quad (82)$$

Furthermore, for  $N_s$  iid uncertainty samples  $\mathbf{w}^{(i)}$ ,  $i \in \mathbb{N}_1^{N_s}$ , let  $\boldsymbol{\sigma}$ ,  $[\boldsymbol{\sigma}]_i = \sigma(\mathbf{w}^{(i)})$ , be the vector of scaling factors determined via Definition 5. Then,  $\Pr [\mathbb{Z}^{\text{S}}(\sigma^*) \subseteq \mathbb{Z}^{\text{P}}] \geq 1 - \varepsilon^c$  holds, where  $\sigma^*$  is the  $N_r$ -th smallest entry of  $\boldsymbol{\sigma}$ , with the discarding parameter  $N_r = \lceil \frac{\varepsilon N_s}{2} \rceil$  and the ceil-function  $\lceil \cdot \rceil$ .

The bound (82) is independent from the number of constraints and dimension of decision variable, and thus lower than the bound defined in (79) in most cases. Furthermore, the complexity of the inner-approximation  $\mathbb{Z}^{\text{S}}(\sigma^*)$  is fully determined by the shape  $\mathbb{Z}^{\text{SAS}}$ . However, it is to note that the conservatism of Proposition 5 depends on how well  $\mathbb{Z}^{\text{SAS}}$  captures the shape of the  $\varepsilon$ -CSS (77), and that for every uncertainty sample an optimization problem needs to

be solved, see (81). Depending on the candidate SAS shape, this optimization problem might be computationally infeasible. A natural candidate for the SAS shape  $\mathbb{Z}^{\text{SAS}}$  is a sampled-polytope SAS  $\tilde{\mathbb{Z}}^{\text{SAS}}$ , akin to (78), constructed with a fixed number  $\tilde{N}_s$  of “design” uncertainty samples  $\tilde{\mathbf{w}}^{(i)}$ ,  $i \in \mathbb{N}_1^{\tilde{N}_s}$ . Thus, the complexity of the shape can be determined apriori by  $\tilde{N}_s$ . For such polytopic SAS, the optimization in (81) can be done efficiently via linear programming. For other possible choices of SAS shapes, we refer to the discussion in [16].

### ACKNOWLEDGMENT

The authors would like to express their gratitude to Julian Berberich for valuable discussions and feedback.

### REFERENCES

- [1] I. Markovsky and F. Dörfler, “Behavioral systems theory in data-driven analysis, signal processing, and control,” *Annual Reviews in Control*, 2021.
- [2] H. Yang and S. Li, “A data-driven predictive controller design based on reduced Hankel matrix,” in *2015 10th Asian Control Conference (ASCC)*, 2015.
- [3] J. Coulson, J. Lygeros, and F. Dörfler, “Data-enabled predictive control: In the shallows of the DeePC,” in *2019 18th European Control Conference (ECC)*, pp. 307–312, IEEE, 2019.
- [4] J. C. Willems, P. Rapisarda, I. Markovsky, and B. L. M. De Moor, “A note on persistency of excitation,” *Systems & Control Letters*, vol. 54, no. 4, pp. 325–329, 2005.
- [5] J. Berberich, J. Köhler, M. A. Müller, and F. Allgöwer, “Data-driven model predictive control with stability and robustness guarantees,” *IEEE Transactions on Automatic Control*, vol. 66, no. 4, pp. 1702–1717, 2021.
- [6] C. Klöppelt, J. Berberich, F. Allgöwer, and M. A. Müller, “A novel constraint-tightening approach for robust data-driven predictive control,” *International Journal of Robust and Nonlinear Control*, 2022.
- [7] G. Pan, R. Ou, and T. Faulwasser, “On a stochastic fundamental lemma and its use for data-driven optimal control,” *IEEE Transactions on Automatic Control*, 2022.
- [8] G. Pan, R. Ou, and T. Faulwasser, “Data-driven stochastic output-feedback predictive control: Recursive feasibility through interpolated initial conditions,” in *Learning for Dynamics and Control Conference*, pp. 980–992, PMLR, 2023.
- [9] S. Kerz, J. Teutsch, T. Brüdigam, M. Leibold, and D. Wollherr, “Data-driven tube-based stochastic predictive control,” *IEEE Open Journal of Control Systems*, vol. 2, pp. 185–199, 2023.
- [10] A. Mesbah, “Stochastic model predictive control: An overview and perspectives for future research,” *IEEE Control Systems Magazine*, vol. 36, no. 6, pp. 30–44, 2016.
- [11] Y. Wang, C. Shang, and D. Huang, “Data-driven control of stochastic systems: An innovation estimation approach,” *arXiv preprint arXiv:2209.08995*, 2022.
- [12] M. Yin, A. Iannelli, and R. S. Smith, “Stochastic data-driven predictive control: Regularization, estimation, and constraint tightening,” *arXiv preprint arXiv:2312.02758*, 2023.
- [13] R. Li, J. W. Simpson-Porco, and S. L. Smith, “Stochastic data-driven predictive control with equivalence to stochastic mpc,” *arXiv preprint arXiv:2312.15177*, 2023.
- [14] M. Farina, L. Giulioni, and R. Scattolini, “Stochastic linear model predictive control with chance constraints—a review,” *Journal of Process Control*, vol. 44, pp. 53–67, 2016.
- [15] M. Lorenzen, F. Dabbene, R. Tempo, and F. Allgöwer, “Stochastic MPC with offline uncertainty sampling,” *Automatica*, vol. 81, pp. 176–183, 2017.
- [16] M. Mammarella, V. Mirasierra, M. Lorenzen, T. Alamo, and F. Dabbene, “Chance-constrained sets approximation: A probabilistic scaling approach,” *Automatica*, vol. 137, p. 110108, 2022.
- [17] M. Mammarella, M. Lorenzen, E. Capello, H. Park, F. Dabbene, G. Guglieri, M. Romano, and F. Allgöwer, “An offline-sampling smpc framework with application to autonomous space maneuvers,” *IEEE Transactions on Control Systems Technology*, vol. 28, no. 2, pp. 388–402, 2018.

- [18] J. Teutsch, S. Kerz, T. Brüdigam, D. Wollherr, and M. Leibold, "Offline uncertainty sampling in data-driven stochastic MPC," *IFAC-PapersOnLine*, vol. 56, no. 2, pp. 650–656, 2023. 22nd IFAC World Congress.
- [19] W. Favoreel, B. De Moor, and M. Gevers, "SPC: Subspace predictive control," *IFAC Proceedings Volumes*, vol. 32, no. 2, pp. 4004–4009, 1999.
- [20] F. Fiedler and S. Lucia, "On the relationship between data-enabled predictive control and subspace predictive control," in *2021 European Control Conference (ECC)*, pp. 222–229, IEEE, 2021.
- [21] R. D. McAllister and J. B. Rawlings, "Nonlinear stochastic model predictive control: Existence, measurability, and stochastic asymptotic stability," *IEEE Transactions on Automatic Control*, vol. 68, no. 3, pp. 1524–1536, 2022.
- [22] T. Sadamoto, "On equivalence of data informativity for identification and data-driven control of partially observable systems," *IEEE Transactions on Automatic Control*, 2022.
- [23] J. Bongard, J. Berberich, J. Köhler, and F. Allgöwer, "Robust stability analysis of a simple data-driven model predictive control approach," *IEEE Transactions on Automatic Control*, vol. 68, no. 5, pp. 2625–2637, 2022.
- [24] I. Markovskiy and P. Rapisarda, "Data-driven simulation and control," *International Journal of Control*, vol. 81, no. 12, pp. 1946–1959, 2008.
- [25] C. De Persis and P. Tesi, "Formulas for data-driven control: Stabilization, optimality, and robustness," *IEEE Transactions on Automatic Control*, vol. 65, no. 3, pp. 909–924, 2019.
- [26] J. Berberich, A. Koch, C. W. Scherer, and F. Allgöwer, "Robust data-driven state-feedback design," in *2020 American Control Conference (ACC)*, pp. 1532–1538, IEEE, 2020.
- [27] A. Alanwar, A. Koch, F. Allgöwer, and K. H. Johansson, "Data-driven reachability analysis from noisy data," *IEEE Transactions on Automatic Control*, 2023.
- [28] J. Berberich, J. Köhler, M. A. Müller, and F. Allgöwer, "On the design of terminal ingredients for data-driven MPC," *IFAC-PapersOnLine*, vol. 54, no. 6, pp. 257–263, 2021.
- [29] S. Kim, R. Pasupathy, and S. G. Henderson, "A guide to sample average approximation," *Handbook of simulation optimization*, pp. 207–243, 2015.
- [30] K. Fukuda, *Polyhedral Computation*. Department of Mathematics, Institute of Theoretical Computer Science ETH Zurich, 2020. Available online: <https://doi.org/10.3929/ethz-b-000426218>.
- [31] L. Martino and J. Míguez, "Generalized rejection sampling schemes and applications in signal processing," *Signal Processing*, vol. 90, no. 11, pp. 2981–2995, 2010.
- [32] H. O. Mete and Z. B. Zabinsky, "Pattern hit-and-run for sampling efficiently on polytopes," *Operations Research Letters*, vol. 40, no. 1, pp. 6–11, 2012.
- [33] M. Lorenzen, M. Cannon, and F. Allgöwer, "Robust MPC with recursive model update," *Automatica*, vol. 103, pp. 461–471, 2019.
- [34] E. Arcari, A. Iannelli, A. Carron, and M. N. Zeilinger, "Stochastic mpc with robustness to bounded parametric uncertainty," *IEEE Transactions on Automatic Control*, 2023.
- [35] F. Blanchini and S. Miani, *Set-theoretic methods in control*. Birkhäuser Boston, MA, 2 ed., 2015.
- [36] H. Schlüter and F. Allgöwer, "Stochastic model predictive control using initial state optimization," *IFAC-PapersOnLine*, vol. 55, no. 30, pp. 454–459, 2022.
- [37] Z.-P. Jiang and Y. Wang, "Input-to-state stability for discrete-time nonlinear systems," *Automatica*, vol. 37, no. 6, pp. 857–869, 2001.
- [38] M. Lorenzen, F. Dabbene, R. Tempo, and F. Allgöwer, "Constraint-tightening and stability in stochastic model predictive control," *IEEE Transactions on Automatic Control*, vol. 62, no. 7, pp. 3165–3177, 2016.
- [39] C. Cai and A. R. Teel, "Input–output-to-state stability for discrete-time systems," *Automatica*, vol. 44, no. 2, pp. 326–336, 2008.
- [40] M. Lazar, W. Heemels, B. Roset, H. Nijmeijer, and P. Van Den Bosch, "Input-to-state stabilizing sub-optimal NMPC with an application to DC–DC converters," *International Journal of Robust and Nonlinear Control*, vol. 18, no. 8, pp. 890–904, 2008.
- [41] M. E. Villanueva, M. A. Müller, and B. Houska, "Configuration-constrained tube MPC," *arXiv preprint arXiv:2208.12554*, 2022.
- [42] T. Alamo, R. Tempo, D. Ramirez, and E. Camacho, "A new vertex result for robustness problems with interval matrix uncertainty," in *2007 European Control Conference (ECC)*, pp. 5101–5107, 2007.
- [43] T. Alamo, R. Tempo, and E. F. Camacho, "Randomized strategies for probabilistic solutions of uncertain feasibility and optimization problems," *IEEE Transactions on Automatic Control*, vol. 54, no. 11, pp. 2545–2559, 2009.